NBS-GCR-85-501

RESPONSE OF COMPLIANT OFFSHORE PLATFORMS TO WAVES

Mircea Grigoriu and Bunu Alibe

School of Civil and Environmental Engineering
Cornell University
Hollister Hall
Ithaca, NY 14853

September 1985

Prepared for
Minerals Management Service
Reston, VA 22091

FOREWORD

The Technology Assessment and Research Branch of the Minerals Management Service (MMS), United States Department of the Interior, is engaged in a program of research and development to provide information on the performance of offshore systems. As part of this program, the MMS is sponsoring the project "Assessment of Uncertainties and Risks Associated with the Dynamic Behavior of Compliant Structures" under contract with the National Bureau of Standards (NBS).

Among these uncertainties are those related to the effects of current and waves on structural response. The purpose of this report is to develop probabilistic descriptors for the response of offshore platforms subjected to such effects. In all cases the study is conducted by using Monte Carlo simulations of the response on the one hand, and statistical linearization techniques on the other. For structures with higher natural frequencies, additional procedures for estimating the response are used as follows. If dynamic effects are negligible (i.e., if the structure responds quasi-statically to the wave excitation), an exact procedure for developing probabilistic descriptors of the response from the probabilistic description of the waves is used, in which it is assumed that the Morison equation holds. If dynamic effects are significant, a time-discretization method is used, which is based on the interpretation of the response as a summation of linear responses due to elemental impulses, and on

the simplified assumption that the forcing function can be described by the Morison equation as applied to a fixed cylinder. To highlight the effect of waves and of the nonlinearities inherent in the damping term of the Morison equation, the report does not include in the calculations the effects of the wind loads on structural response, and assumes a value of the drag coefficient in the Morison equation which, for structures of the Tension Leg Platform Type, is relatively large ($C_d = 1.0$). The comparisons presented in the report show that the mean peak response and the mean upcrossing rates corresponding to various response levels calculated by statistical linearization techniques are, under these conditions, generally smaller than the response obtained by simulation (or by the procedures proposed in the report). The conclusions of the report thus suggest that statistical linearization techniques should not be applied uncritically, and that the extent to which they are acceptable should be verified carefully for each design situation.

Emil Simiu
Structures Division
Center for Building Technology
National Bureau of Standards

DISCLAIMER

The statements and conclusions contained in this report are those of the contractor and do not necessarily reflect the view of the U.S. Government and, in particular, the National Bureau of Standards or the Department of the Interior. Neither NBS or the contractors make any warranty, express or implied, or assume any legal liability or responsibility for the accuracy, completeness or usefulness of any information, apparatus, product or process disclosed or represent that its use would not infringe privately owned rights. They accept no responsibility for any damage that may result from the use of any information contained herein. The mentioning of manufacturers, professional firms, names, products, and the publication of performance data do not constitute any evaluation or endorsement by the U.S. Government, its agencies, or the contractor. It is done in a generic sense to illustrate particular points.

ABSTRACT

Probabilistic descriptors are developed for the response of structures of the Tension Leg Platform type to current and waves. These are obtained by Monte Carlo techniques by assuming the validity of the Morison equation. The results are compared to those obtained by using statistical linearization techniques. Also, for offshore platforms with higher natural periods of vibration, mean upcrossing rates for various levels of the structural response are estimated by simulation, by statistical linearization techniques, and by additional procedures developed in the report. It is concluded that statistical linearization techniques can underestimate significantly the structural response induced by current and waves.

RESPONSE OF COMPLIANT OFFSHORE PLATFORMS TO WAVES

By Mircea Grigoriu and Bunu Alibe

INTRODUCTION

Wave forces are generally modeled by the Morison equation and involve two components, the drag force and the inertia force (7,8). These forces depend on wave particle velocity, wave particle acceleration, and structural motion. The dependence on structural motion can be significant for structures with large periods of vibration, such as Tension Leg Platforms. The period of vibration of these offshore platforms is of the order of 100 sec.

This study develops probabilistic descriptors for the response of platforms of the Tension Leg type. First, the statistical linearization method is evaluated based on a simplified single degree of freedom mechanical model considered previously for the surge motion of compliant platforms (14). Then, the surge and pitch response of a realistic Tension Leg Platform are studied. The analysis accounts in this case for the spatial correlation of wave forces.

SURGE MOTION

Let R(t) be the surge response of a hypothetical platform consisting of a cylindrical member with diameter d and area $A = \frac{\pi d^2}{4}$. Following Ref. 15, it is assumed that R(t) satisfies the differential equation

$$\ddot{R}(t) + 2\zeta\omega_o \dot{R}(t) + \omega_o^2 R(t) = \frac{\rho A}{m} \ddot{R}(t) + \frac{C_M \rho A}{m} (\dot{U}^*(t) - \ddot{R}(t)) + \frac{1}{2} \frac{C_D \rho d}{m} (U^*(t) - \dot{R}(t)) \, |U^*(t) - \dot{R}(t)| \tag{1}$$

in which m, ζ, and ω_o = the mass, the damping ratio, and the natural frequency of vibration of the platform. Since the nonlinearity in the restoring

force has relatively small effects on response (13), the restoring force is considered to be proportional with R(t). Second order effects and convective acceleration terms in the wave force are not included in the analysis. The wave forces are modeled by the Morison equation and depend on the drag and inertia coefficients, c_D and c_M, structural response, and wave characterstics. The wave particle velocity process

$$U^*(t) = u_o + U(t) \tag{2}$$

is a stationary Gaussian process with mean (current) u_o and variance σ_U^2. The one-sided power spectral density of U(t) is

$$G_U(\omega) = \begin{cases} \dfrac{c_1}{\omega^3} \exp\left(-\dfrac{c_2}{v^4\omega^4}\right) & , \quad 0 \leq \omega \leq \bar{\omega} \\ 0.0 & , \quad \omega > \bar{\omega} \end{cases} \tag{3}$$

because, according to the linear wave theory, G_U can be obtained at free water surface by multiplying the ordinates of sea elevation spectrum with ω^2. This spectrum coincides with the Pierson-Moskowitz spectrum in the range $[0,\bar{\omega}]$ and depends on the constants $c_1 = 0.78\ m^2/sec^4$; $c_2 = 6.85 \times 10^3\ m^4/sec^8$, and the wind speed v measured in m/sec. (8,9,10). The cutoff frequency $\bar{\omega}$ is usually assumed to be $3\omega_p$, in which ω_p = the frequency at which the spectrum takes on its maximum value (6). Note that the process U(t) can be differentiated indefinitely when $\bar{\omega} < \infty$. On the other hand, U(t) is not differentiable when $\bar{\omega}$ is unbounded or, equivalently, G_U in Eq. 3 coincides with Pierson-Moskowitz spectrum. The power spectral density of U(t) at any water depth can be determined from the spectrum in Eq. 3 scaled by a depth attenuation factor (10). The wave force in Eq. 1 is the resultant of the water pressures acting on the platform.

The analysis is based on two methods: statistical linearization and

simulation. It is shown that the statistical linearization method can underestimate significantly the peak response of compliant platforms. This limitation of the statistical linearization method is primarily caused by the implicit assumption in this method that the response follows a Gaussian distribution.

Similar limitations of the statistical linearization method are presented in Appendix A for stiffer offshore structures with periods smaller than 16 seconds. Such structures respond either dynamically or quasi-statically to wave forces. The report and the Appendix can be read independently.

Statistical Linearization Method

The method has been applied extensively to analyze complex dynamic systems, particularly for the estimation of the second-moment descriptors of the response, e.g., the mean and variance (11,14). Recently, the method was employed to find the mean and variance of the response of offshore structures to wave forces characterized by the motion dependent form of the Morison model in Eq. 1 (14).

The statistical linearization method is based on the assumption that the solution R(t) of Eq. 1 can be approximated by the solution $R_L(t)$ of the linear differential equation

$$\ddot{R}_L(t) + 2\,\zeta^*\,\omega_o^*\,\dot{R}_L(t) + \omega_o^{*2}\,R_L(t) = W^*(t) \qquad (4)$$

in which ζ^* = an effective damping ratio accounting for nonlinearities in Eq. 1, ω_o^* = a modified natural frequency depending on ω_o, structural mass m, and the added mass $c_I\,\rho A$ in which $c_I = c_M - 1$, and $W^*(t)$ = the effective wave load process. Since $W^*(t)$ is a linear function of U(t), the approximate response $R_L(t)$ is a Gaussian process. However, the distribution of R(t) can differ from the Gaussian distribution (4,5). The approximating linear

differential equation of motion can be obtained by minimizing an expected error (11,14).

Simulation Method

Figure 1 shows a discrete approximation of the power spectral density in Eq. 3. According to this approximation, U(t) has power at N frequencies ω_i which can be measured by the variances σ_i^2. The process can be represented by

$$U(t) = \sum_{i=1}^{N} (A_i \cos \omega_i t + B_i \sin \omega_i t) \qquad (5)$$

in which A_i and B_i are zero-mean, mutually independent Gaussian variables (2,11). The variance of A_i and B_i is σ_i^2. From Eq. 5, the wave particle acceleration has the expression

$$\dot{U}(t) = \sum_{i=1}^{N} \omega_i (- A_i \sin \omega_i t + B_i \cos \omega_i t) \qquad (6)$$

The simulation method involves three phases. First, realizations of U(t) and $\dot{U}(t)$ are generated over any storm duration τ from Eqs. 5 and 6 and samples of $\{A_i, B_i\}$, i = 1, ..., N. These realizations provide samples of the wave force process in Eq. 1. Second, deterministic dynamic analyses are performed to determine the response in $(0,\tau)$ to these samples. The analyses involve time-domain integrations and determinations of the peak response in τ, the rate of exceedings (upcrossings) of specified (strength) thresholds, and other response descriptors for every sample of the wave force process. Third, the sample response descriptors are used to calculate means and variances of the response, the average peak response in τ, and mean upcrossing rates.

Numerical Results

Means, variances, and mean rates at which the response exceeds specified thresholds (mean upcrossing rates) are determined by statistical

linearization and simulation for the model in Eq. 1. These descriptors can be calculated simply for linearized stationary responses because the approximate responses follow Gaussian distributions. For example, the mean upcrossing rate of level r of $R_L(t)$ is (3)

$$\nu_L(r) = \frac{1}{2\pi} \frac{\dot{\sigma}_L}{\sigma_L} \exp\left[-\frac{1}{2}\left(\frac{r-m_L}{\sigma_L}\right)^2\right] \tag{7}$$

in which m_L and σ_L = the mean and the standard deviation of $R_L(t)$ and $\dot{\sigma}_L$ = the standard deviation of $\dot{R}_L(t)$.

Table 1 gives structural characteristics and wave parameters considered in analysis. Table 2 provides response descriptors obtained by statistical linearization and simulation. The simulation analysis involves, e.g., N = 2048 equally spaced frequencies (Eqs. 5 and 6) over the range (0,4.7) rad/sec for a wind speed v = 30 m/s and is based on 100 samples with length of approximately one hour. The integration of Eq. 1 uses a time step Δ = 0.67 sec.

From Table 2, the statistical linearization method provides satisfactory approximations only for the mean response. Both the standard deviation and the mean upcrossing rate function are underestimated significantly. Figure 2 shows the variation with α of averages of the peak response obtained by simlation and statistical linearization for various wind speeds and a storm duration of approximately one hour. From this figure and Table 2, the statistical linearization method generally underestimates the mean peak response. Note also that mean peak responses predicted by this method increase slowly with the current ratio α. The unsatisfactory performance of the statistical linearization method is caused primarily by the relatively rapid increase of the effective damping ratio ζ^* in Eq. 4 with α, the implicit assumption that the response is a Gaussian process, and the inaccurate representation of the excitation particularly in the low frequency range. In this frequency range,

the power spectral density of the effective load force $W^*(t)$ in Eq. 4 is nearly zero. However, the actual forces have power in the low frequency range.

SURGE AND PITCH MOTION

Consider the Tension Leg Platform in Fig. 3(a) with mechanical and geometrical characteristics in Table 3. The platform has four 15 m diameter columns connected by horizontal beams (pontoons) of diameter 7.5 m. It is subjected to spatially correlated wave forces acting in the x direction and oscillates in the (x,z)-plane. For dynamic analysis, the platform is idealized as a rigid body with two degrees of freedom: the surge and the pitch, as shown in Fig. 3(b). Let $R_X(t)$ and $R_\theta(t)$ be the structural displacement in the x direction and the rotation about the mass center, i.e., the surge and the pitch motions.

The response vector $\underline{R}(t) = \{R_X(t), R_\theta(t)\}$ satisfies the differential equation

$$\underline{m}\,\ddot{\underline{R}}(t) + \underline{c}\,\dot{\underline{R}}(t) + \underline{k}\,\underline{R}(t) = \underline{W}(t) \tag{8}$$

in which the components $W_X(t)$ and $W_\theta(t)$ of the wave force vector $\underline{W}(t)$ are the resultant in the x-direction and the moment about the structural mass center of the elementary wave forces acting at all points of the platform. These elementary forces have the same functional form as in Eq. 1. The mass and stiffness matrices, $\underline{m}$ and $\underline{k}$, are

$$\underline{m} = \begin{bmatrix} m & 0 \\ 0 & I \end{bmatrix} = \begin{bmatrix} 4.03\times10^{6}\ \text{kg} & 0 \\ 0 & 8.45\times10^{9}\ \text{kg-m}^2 \end{bmatrix}$$

$$\underline{k} = \begin{bmatrix} k_{XX} & k_{X\theta} \\ k_{\theta X} & k_{\theta\theta} \end{bmatrix} = \begin{bmatrix} 33.78\ \text{kN/m} & 1.28\times10^{3}\ \text{kN} \\ 1.28\times10^{3}\ \text{kN} & 1.53\times10^{11}\ \text{kNm} \end{bmatrix} \tag{9}$$

in which m = the total structural mass, I = the mass moment of inertia about an axis perpendicular to the (x,z) plane at the mass center, and k_{xx}, $k_{x\theta}$, $k_{\theta x}$, and $k_{\theta\theta}$ = the stiffness associated with the surge and pitch. These stiffnesses can be determined from characteristics of the platform in Table 3.

The analysis is based on simulation and involves the same steps as in the solution of Eq. 1. However, in this case, both the numerical integration of the equation of motion and the generation of wave force samples are less simple. The numerical integration is based on modal decomposition and the assumption that $\underline{\dot{R}}(t)$ can be approximated at any t by its value at the previous time step (1). The damping structural characteristics correspond to 5% of the modal critical damping ratios. The generation of wave force samples accounts for the spatial correlation between waves acting at various structural points. This correlation results from the spatial pattern of the wave particle velocity process, which can be characterized by the cross-spectrum of this process. The one-sided cross-spectrum between the velocities $U_p(t)$ and $U_q(t)$ in the x-direction at points p and q of coordinates (x_p,z_p) and (x_q,z_q) is assumed to be (12)

$$G_{pq}(\omega) = \omega^2 \, G_U(\omega) \, \Lambda \, (\omega;\, z_p,\, z_q) \exp\left[-\sqrt{-1}\; r\; (x_p - x_q)\right] \qquad (10)$$

in which G_U is defined in Eq. 3, r = the wave number which can be determined according to the deep water aproximation as the ratio between the square of the frequency and the constant of gravity g, h = the ocean depth, z = the elevation from the sea floor, and

$$\Lambda \, (\omega;\, z_p,\, z_q) = \frac{\cosh\,(r\, z_p)\, \cosh\,(r z_q)}{\sinh^2\,(rh)} \qquad (11)$$

Consider P structural points and let $\underline{U}(t)$ be the vector of wave particle velocities $\{U_p(t)\}$, p = 1, 2, ..., P, at these points. If the spectra G_{pq} in Eq. 9 are discretized and their power is concentrated at N frequencies $\{\omega_i\}$,

i = 1, 2, ..., N, $\underline{U}(t)$ can be represented by the sum of harmonics

$$\underline{U}(t) = \sum_{i=1}^{N} (\underline{A}_i \cos \omega_i t + \underline{B}_i \sin \omega_i t) \qquad (12)$$

in which $\underline{A}_i$ and $\underline{B}_j$ are zero-mean independent Gaussian vectors for any i and j. The covariance matrices of these vectors are $E[\underline{A}_i \underline{A}_i^T] = E[\underline{B}_i \underline{B}_i^T] = \{\gamma_{pq}^i\}$, p, q = 1, 2, ..., P, and i = 1, 2, ..., N, where $\gamma_{pq}^i = G_{pq}(\omega_i)\ \Delta\omega_i$ and $\Delta\omega_i$ = the frequency interval associated with ω_i. Equation 12 can be applied directly to generate spatially correlated wave particle velocity processes from realizations of the Gaussian vectors $\underline{A}_i$ and $\underline{B}_i$. The use of Fast Fourier Transform algorithms increases significantly the efficiency of the procedure.

Table 4 gives means, standard deviations, and averages of the peak response in storms of duration $\tau \simeq 0.7$ hours for several wind speeds and current ratios $\alpha = u_o/\sigma_U$. Note that the pitch response has minor effects on the tension in the platform legs. For example, the variation in the initial tension in tethers is less than 1% for the average peak pitch response corresponding to v = 45 m/s and $\alpha = 1.0$. Additional runs based on the single degree of freedom model in Eq. 1 showed that the surge response can be estimated independently of the pitch motion. The analysis assumes the cross spectrum in Eq. 10 and a linear variation of the current from zero at the ocean floor to u_o at the free water level. The wave force vector $\underline{W}(t)$ is determined approximately by concentrating the wave forces at 3 points along each column of the platform.

CONCLUSIONS

Probabilistic descriptors were developed for the surge and pitch responses of Tension Leg Platforms to random wave forces. The platforms were assumed to behave linearly and the wave forces were characterized by

a motion dependent form of the Morison equation. The analysis was based on statistical linearization and simulation and has accounted for the spatial correlation of the wave force process.

It was found that the statistical linearization method provides inaccurate estimates of the response which are generally on the unconservative side. The use of the method in the analysis of Tension Leg Platforms can result in unsafe designs. The proposed simulation method is efficient and can account for the spatial pattern of waves.

REFERENCES

1. Anagnostopoulos, S. A., "Dynamic Response of Offshore Platforms to Extreme Waves Including Fluid-Structure Interaction," Engineering Structures, Vol. 4, July, 1982, pp. 179-185.

2. Borman, L. E., "Ocean Wave Simulation for Engineering Design," Journal of Waterways and Harbors Division, ASCE, Vol. 95, No. WW4, November, 1969, pp. 557-583.

3. Cramer, H., and Leadbetter, M. R., Stationary and Related Stochastic Processes, John Wiley & Sons, New York, 1967.

4. Grigoriu, M., and Alibe, B., "Practical Approximations of Peak Wave Forces," Research Report NBS-GCR-84-481, National Bureau of Standards, November 1984.

5. Grigoriu, M., "Extremes of Wave Forces," Journal of Engineering Mechanics Division, ASCE, Vol. 110, No. 12, December 1984, pp. 1731-1742.

6. Hallam, M. G., Heaf, N. J., and Wootton, L. R., Dynamics of Marine Structures: Methods of Calculating the Dynamic Response of Fixed Structures Subject to Wave and Current Action, CIRIA Under Water Engineering Group, Report UR8, London, October, 1978.

7. Moe, G., "Long-Term Wave-Force Statistics for a Vertical Pile," Coastal Engineering, Vol. 2, 1979, pp. 297-311.

8. Morison, J. R., O'Brien, M. P., Johnson, J. W., and Schaff, S. A., "The Force Exterted by Surface Waves on Piles," Petroleum Transactions, American Institute of Mining Engineers, Vol. 189, 1950, pp. 149-154.

9. Pierson, W. J., and Moskowitz, L., "A Proposed Spectrum Form for Fully Developed Wind Seas Based on the Similarity Theory of S. A. Kitaigorodskii," Journal of Geophysical Research, Vol. 69, No. 24, December, 1964, pp. 5181-5190.

10. Sarpakaya, T., and Isaacson, M., Mechanics of Wave Forces on Offshore Structures, Van Nostrand Reinhold Company, New York, 1981.

11. Shinozuka, M., "Monte Carlo Solution of Structural Dynamics," Computers and Structures, Vol. 2, 1972, pp. 855-873.

12. Sigbjorusson, R., and Morch, M., "Spectral Analysis of Nonlinear Wave Load Effects on Offshore Platforms," Engineering Structures, Vol. 4, January, 1982, pp. 29-36.

13. Simiu, E., and Leigh, S. D., "Turbulent Wind Effects on Tension Leg Platform Surge," NBS Building Science Series 151, U.S. Department of Commerce, March 1983.

14. Soong, T. T., Random Differential Equations in Science and Engineering, Academic Press, New York, 1973.

15. Spanos, P.-T. D., and Chen, T. W., "Random Response to Flow-Induced Forces," Journal of Engineering Mechanics, ASCE, Vol. 107, No. 6, Dec. 1981, pp. 1173-1190.

Table 1. Structure and Wave Parameters

Parameters	Values
m	8.575×10^6 kg
ζ	5%
ω_o	0.06 rad/sec.
d	18m
ρ	1000 kg/m^3
C_D	1.0
C_M	2.0

Table 2. Probabilistic Characteristics of Response

Response Descriptors		v = 15 m/s			v = 30 m/s			v = 45 m/s		
		α=0.0 u_o=0.0	α=0.5 u_o=0.49m/s	α=1.0 u_o=0.97m/s	α=0.0 u_o=0.0	α=0.5 u_o=0.97m/s	α=1.0 u_o=1.94m/s	α=0.0 u_o=0.0	α=0.5 u_o=1.46m/s	α=1.0 u_o=2.91m/s
Mean (meters)	Statistical Linearization, m_L	0.000	0.216	0.472	0.000	0.838	1.887	0.000	1.880	4.238
	Simulation, m	0.000	0.219	0.496	0.001	0.885	2.001	-0.001	1.997	4.472
Standard Deviation (meters)	Statisical Linearization, σ_L	0.071	0.071	0.071	0.294	0.295	0.299	0.727	0.739	0.779
	Simulation, σ	0.240	0.246	0.296	0.539	0.749	1.015	1.219	1.689	2.311
Mean Peak Response (meters)	Statistical Linearization	0.45	0.55	0.71	1.76	2.06	2.56	6.70	6.72	6.75
	Simulation	1.03	1.16	1.56	2.01	3.49	5.35	4.36	7.85	12.46
Ratios of Mean Upcrossing Rates ν/ν_L	$\tilde{r}$ = 1	6.39×10	1.45×10^{2}	4.40×10^{3}	1.81	9.35	4.16×10^{3}	1.49	5.59	4.66×10
	$\tilde{r}$ = 2	3.73×10^{8}	3.67×10^{9}	7.19×10^{14}	5.73×10	5.03×10^{4}	3.29×10^{14}	2.23×10	4.98×10^{3}	1.61×10^{7}
	$\tilde{r}$ = 3	2.19×10^{20}	1.28×10^{22}	3.75×10^{33}	3.67×10^{4}	8.92×10^{10}	2.04×10^{32}	3.39×10^{3}	4.53×10^{8}	2.27×10^{16}
	$\tilde{r}$ = 4	---	---	---	9.38×10^{8}	1.39×10^{20}	---	5.41×10^{6}	5.87×10^{15}	7.89×10^{28}

Notes: (1) $\tilde{r} = (r - m)/\sigma$ = standardized threshold;
(2) $\alpha = u_o/\sigma_U$ = current ratio;
(3) ζ = critical damping ratio = 5%;
(4) ν_L and ν = mean upcrossing rates obtained by stabilized linearization and simulation, and
(5) "---" if $\nu_L \approx 0.0$.

Table 3. Mechanical and Geometrical Characteristics of the Tension Leg Platforms in Fig. 3

Parameter	Value
Column Diameter	15 m
Pontoon Diameter	7.5 m
Deck Mass, m	40×10^5 kg
Water Depth, h	450 m
Tension in Tethers	14,000 kN
Tethers Length	415 m

Table 4. Surge and Pitch Response of Tension Leg Platforms

Response Descriptors	v = 15 m/s			v = 30 m/s			v = 45 m/s		
	α=0.0 u_o=0.0	α=0.5 u_o=0.49m/s	α=1.0 u_o=0.97m/s	α=0.0 u_o=0.0	α=0.5 u_o=0.97m/s	α=1.0 u_o=1.94m/s	α=0.0 u_o=0.0	α=0.5 u_o=1.46m/s	α=1.0 u_o=2.91m/s
Surge Response									
Mean (m)	0.0007	1.3286	3.483	0.022	8.45	19.14	-0.011	20.78	45.41
Standard Deviation (m)	1.073	1.204	1.457	7.140	9.22	12.46	27.32	32.11	41.02
Mean Peak Response (m)	4.71	6.04	9.04	26.17	42.10	63.67	95.94	146.29	198.30
Pitch Response									
Mean (rad)	-3.50×10^{-9}	-1.63×10^{-5}	-4.36×10^{-5}	1.88×10^{-7}	-1.07×10^{-4}	-2.43×10^{-4}	-1.34×10^{-7}	-2.65×10^{-4}	-5.80×10^{-4}
Standard Deviation (rad)	8.93×10^{-5}	9.13×10^{-5}	9.17×10^{-5}	2.74×10^{-4}	2.81×10^{-4}	3.05×10^{-4}	4.15×10^{-4}	4.53×10^{-4}	5.26×10^{-4}
Mean Peak Response (rad)	3.19×10^{-4}	3.08×10^{-4}	2.74×10^{-4}	1.07×10^{-3}	8.76×10^{-4}	7.24×10^{-4}	1.59×10^{-3}	1.37×10^{-3}	1.16×10^{-3}

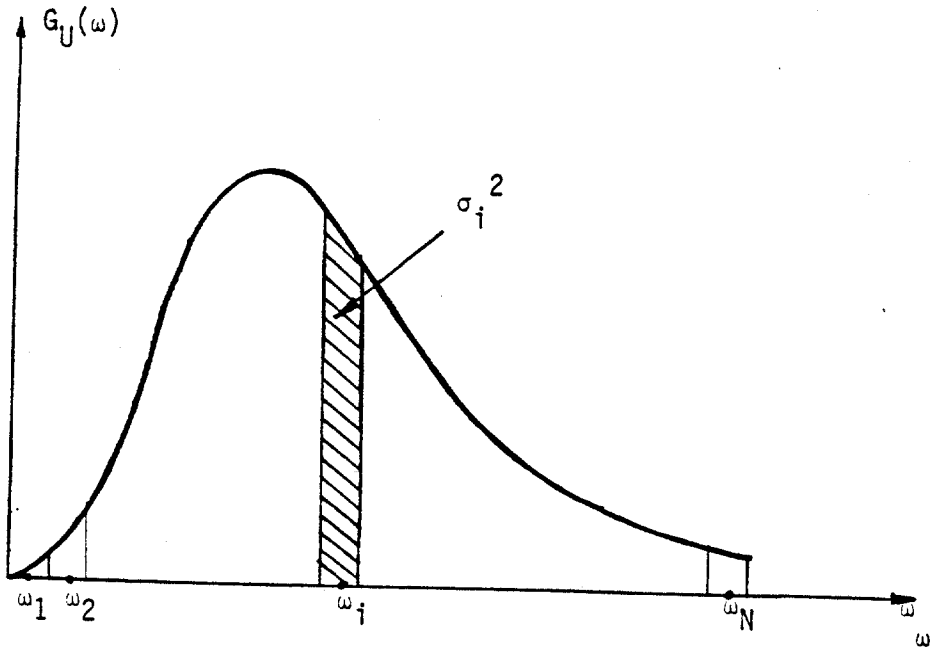

Figure 1. Discrete Approximation of Mean Power Spectral Density.

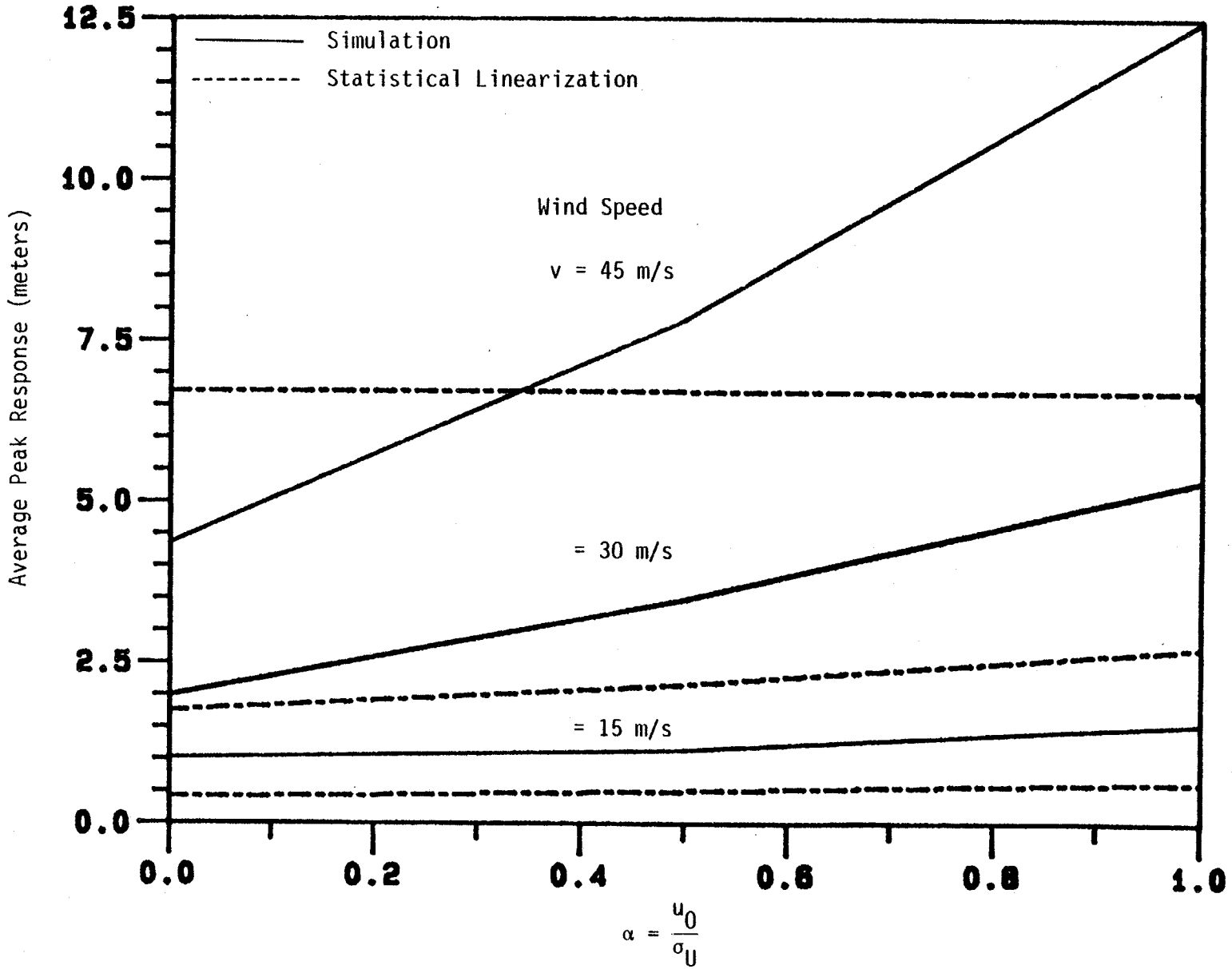

Figure 2. Average Peak Surge Response

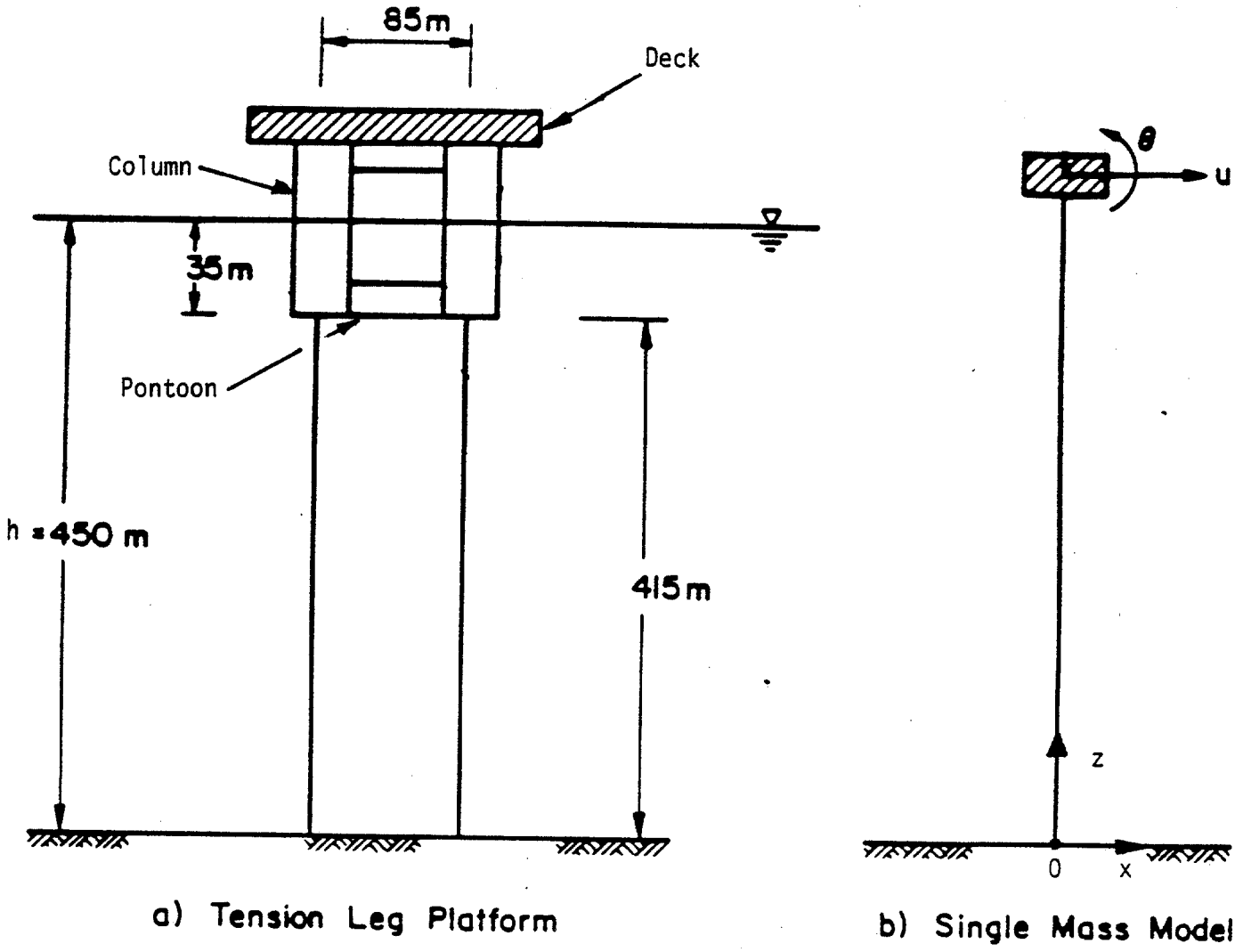

Figure 3. Tension Leg Platform

APPENDIX A

ABSTRACT

Probability density functions, mean crossing rates, and other descriptors are developed for the quasi-static and dynamic reponses of offshore platforms to wave forces. It is assumed that offshore platforms can be modeled by simple oscillators, the wave particle velocity is a stationary differentiable Gaussian process, the Morison's equation can be applied, and wave forces are perfectly correlated spatially. Results show that both the quasi-static response and the dynamic response of offshore platforms to wave forces are generally underestimated if the drag force is linearized. Estimates are developed for probabilistic characteristics of these responses based on the crossing theory of random processes and time-discretization of the wave force process. Simulation studies indicate that these estimates are satisfactory.

KEY WORDS

Crossing Theory, Morison's equation, Offshore Structures, Probability Theory, Random Processes, Wave Forces

RESPONSE OF OFFSHORE STRUCTURES TO RANDOM WAVES

By Mircea Grigoriu*, M.ASCE, and Bunu Alibe**

INTRODUCTION

Wave forces are generally modeled by the Morison's equation and involve two components, the drag force and the inertia force (18,20). The response of offshore structures to wave forces can be quasi-static or dynamic depending on the mechanical characteristics of these structures and the frequency content of the waves. The quasi-static response of linear structures is particularly simple to determine because it is approximately proportional to the excitation. Thus, probabilistic characteristics of this response can be obtained directly from those of the wave force (5,6,7). On the other hand, the dependence of dynamic responses on excitation is less simple. Statistical linearization or other approximations (10,22,23) and simulation studies (3,21) are generally employed to analyze dynamic responses.

This paper develops analytical methods for the determination of the mean (failure) rate at which the response exceeds structural strength and other response descriptors for both quasi-static and dynamic oscillations of offshore structures subject to waves. The mean failure rate is determined exactly for quasi-static responses and approximately for dynamic responses. Simulation is employed to evaluate the statistical linearization method and other approximations. It is assumed that the offshore structures can be modeled by simple linear oscillators. The Morison's equation is applied to represent wave forces.

WAVE FORCES

Let

* Assoc. Professor of Civil Engineering, Cornell University, Ithaca, NY 14853
** Grad. Student of Civil Engineering, Cornell University, Ithaca, NY 14853

$$U^*(t) = u_0 + U(t) \tag{1}$$

be the wave particle velocity, in which the current u_0 is deterministic and the fluctuating component U(t) follows a stationary Gaussian process with zero mean and one-sided mean power spectral density

$$G_U(\omega) = \begin{cases} \dfrac{c_1}{\omega^3} \exp\left(-\dfrac{c_2}{v^4\omega^4}\right) & , \quad 0 \leq \omega \leq \bar{\omega} \\ 0 & , \quad \omega > \bar{\omega} \end{cases} \tag{2}$$

This spectrum coincides with the Pierson-Moskowitz spectrum (20) in the range $[0, \bar{\omega}]$ and depends on the constants $c_1 = 8.4$ ft^2/sec^4; $c_2 = 8.0\text{x}10^5$ ft^4/sec^8 and the wind speed v measured in ft/s. The cutoff frequency $\bar{\omega}$ is usually larger than $3\,\omega_p$, in which ω_p = the frequency at which the spectrum takes on its maximum value (16). The process U(t) can be differentiated indefinitely when $\bar{\omega} < \infty$. Denote by σ_U, $\sigma_{\dot{U}}$, and $\sigma_{\ddot{U}}$ the standard deviations of U(t), $\dot{U}(t) = dU(t)/dt$, and $\ddot{U}(t) = d^2U(t)/dt^2$ in this case. On the other hand, U(t) is not differentiable when $\bar{\omega}$ is unbounded or, equivalently, $G_U(\omega)$ in Eq. 2 coincides with the Pierson-Moskowitz spectrum.

Figure 1 shows the spectrum in Eq. 2 for several values of the wind speed v. The power of U(t) increases with the wind speed v but changes its distribution along the frequency axis. For example, the peak of $G_U(\omega)$ is at approximately 0.7 rad/s for v = 50 ft/s and 0.3 rad/s for v = 100 ft/s. In addition to the Pierson-Moskowitz spectrum, other spectra have been proposed for the wave particle velocity process, e.g., the JONSWAP spectrum which was developed for conditions prevalent in the North Sea (20).

Wave forces are modeled in this paper by various forms of the Morison's equation which disregard or account for flow-structure interaction. In all cases, wave loadings consist of the superposition of two components, drag

forces and inertia forces. Drag forces depend nonlinearly on $U^*(t)$ while inertia forces are linearly related to $\dot{U}^*(t)$. Note that inertia forces are defined only when the wave particle velocity is a differentiable process or $\bar{\omega} < \infty$ in Eq. 2.

The non-interactive Morison equation for fixed cylindrical members is

$$X(t) = a_1 X_1 + a_2 X_2(t) \tag{3}$$

in which $a_1 X_1(t)$ = the drag force, $a_2 X_2(t)$ = the inertia force,

$$\begin{aligned} X_1(t) &= U^*(t) \left|U^*(t)\right| \\ X_2(t) &= \dot{U}^*(t) = \dot{U}(t) \end{aligned} \tag{4}$$

and

$$\begin{aligned} a_1 &= \frac{1}{2} c_d \rho d \\ a_2 &= c_m \rho \frac{\pi d^2}{4} \end{aligned} \tag{5}$$

The parameters a_1 and a_2 depend on the diameter of the cylindrical member d, the flow density ρ, and the drag and inertia coefficients c_d and c_m. The coefficients take on values in the ranges (0.6, 1.0) and (1.5, 2.0), respectively (1).

The interactive forms of the Morison equation involve time derivatives of the structural displacement process R(t). For example, according to the relative velocity model, the wave force is (14,20).

$$Y(t) = a_1 \left(U^*(t)-\dot{R}(t)\right) \left|U^*(t)-\dot{R}(t)\right| + a_2 \left[\dot{U}^*(t) - \left(1 - \frac{1}{c_m}\right) R(t)\right] \quad (6)$$

On the other hand, the wave force predicted by the independent field model has the form (17)

$$Z(t) = X(t) - a_1 \dot{R}(t) \left|\dot{R}(t)\right| - a_2 \left(1 - \frac{1}{c_m}\right) R(t) \quad (7)$$

The models in Eqs. 6 and 7 have been developed for the analysis of flexible structures, such as tension leg platforms. For these structural systems, the flow-structure interaction is a major source of additional damping. Previous studies (2,9) show that Eq. 3 can be applied even to the analysis of flexible offshore platforms, provided that the structural damping is increased to account for effects of flow-structure interaction. This additional damping is referred to as hydrodynamic damping and can be estimated from comparisons of offshore platform responses to the interactive and noninteractive wave forces in Eqs. 3, 6, and 7.

QUASI-STATIC RESPONSE

Consider a simple oscillator with natural frequency much larger than the frequencies of the excitation. The oscillator response is practically proportional to the excitation and is referred to as quasi-static response.

This section examines the quasi-static response of offshore structures to the non-interactive form of the Morison equation. From Eq. 3,

$$R(t) = \frac{1}{k} \left[a_1 X_1(t) + a_2 X_2(t)\right] \quad (8)$$

in which k = the structural stiffness. The distribution of the peak response during any period τ can be approximated by (8,26).

$$F_\tau(r) \simeq \exp\,(-\,\nu(r)\,\tau) \tag{9}$$

in which $\nu(r)$ is the mean rate at which R(t) crosses from below (upcrosses) a strength level r. $\nu(r)$ can be obtained from the mean (outcrossing) rate at which the vector process $\underline{\xi}(t) = \{\xi_1(t),\ \xi_2(t)\}^T$ leaves the bivariate safe domain $D = \{(\xi_1,\ \xi_2):\ \xi_1 + \xi_2 < \xi\}$, in which

$$\begin{aligned}
&\xi_1(t) = X_1(t) = \left(u_0 + U(t)\right)\left|u_0 + U(t)\right| \\
&\xi_2(t) = a\,X_2(t) = a\,\dot{U}^*(t) = a\,\dot{U}(t) \\
&\xi = kr/a \\
&a = a_2/a_1
\end{aligned} \tag{10}$$

The mean outcrossing rate of $\underline{\xi}(t)$ relative to D is (24)

$$\nu(r) = \int_L d\underline{\xi}\ E\left[\dot{\xi}_n(t) + \,/\, \underline{\xi}(t) = \underline{\xi}\right] f(\underline{\xi}) \tag{11}$$

in which f = the first order density of $\underline{\xi}(t)$ and

$$E\left[\dot{\xi}_n(t) + \,/\, \underline{\xi}(t) = \underline{\xi}\right] = \int_0^\infty \dot{\xi}_n\, f(\dot{\xi}_n \,/\, \underline{\xi})\, d\dot{\xi}_n \tag{12}$$

is the expectation of the positive tail of the projection of $\dot{\underline{\xi}}(t)$ on the exterior normal $\underline{n} = \left(\frac{1}{\sqrt{2}}, \frac{1}{\sqrt{2}}\right)$ to the limit state $L = \{(\xi_1,\ \xi_2) : \xi_1 + \xi_2 = \xi\}$ given that $\underline{\xi}(t) = \underline{\xi}$ on L. The conditional density $f(\dot{\xi}_n/\underline{\xi})$ in Eq. 12 can be

obtained by differentiating the conditional probability $F(\dot{\xi}_n/\underline{\xi}) = P\left(\dot{\xi}_n(t) < \dot{\xi}_n \;/\; \xi_1(t) = \xi_1,\ \xi_2(t) = \xi - \xi_1\right)$ with respect to $\dot{\xi}_n$. This probability depends on the processes $\xi_1(t)$ and $\xi_2(t)$ in Eq. 10 and their derivatives

$$\begin{aligned} \dot{\xi}_1(t) &= 2\left|u_0 + U(t)\right| \dot{U}(t) \\ \dot{\xi}_2(t) &= a\, U(t) \end{aligned} \tag{13}$$

because

$$\dot{\xi}_n(t) = \frac{1}{\sqrt{2}}\left(\dot{\xi}_1(t) + \dot{\xi}_2(t)\right) \tag{14}$$

From Eqs. 10, 13, and 14,

$$F(\dot{\xi}_n/\underline{\xi}) = P\left(\frac{2\left|u_0+U(t)\right|\dot{U}(t)+a\,U(t)}{\sqrt{2}} < \dot{\xi} \quad / \quad \begin{matrix} \left(u_0+U(t)\right)\left|u_0+U(t)\right| = \xi_1 \\ \dot{U}(t) = (\xi - \xi_1)/a \end{matrix}\right) \tag{15}$$

Elementary calculations show that the first condition implies that $\left|u_0 + U(t)\right| = \sqrt{\left|\xi_1\right|}$ and the conditional variable $U(t) \;/\; \dot{U}(t) = u$ follows a Gaussian distribution with mean $-\left(\sigma_{\dot{U}}^2 \;/\; \sigma_U^2\right)u$ and variance $\sigma_U^2 - \sigma_{\dot{U}}^4 \;/\; \sigma_U^2$. As a result,

$$F(\dot{\xi}_n/\underline{\xi}) = \Phi\left(\frac{\sqrt{2}\,\dot{\xi}_n\, a - b}{c}\right) \tag{16}$$

and

$$f(\dot{\xi}_n/\xi) = \frac{\sqrt{2}\,a}{c}\,\phi\left(\frac{\sqrt{2}\,\dot{\xi}_n\,a - b}{c}\right) \tag{17}$$

in which,

$$b = 2\sqrt{|\xi_1|}\,(\xi - \xi_1) - \frac{\sigma_{\dot{U}}^2\,a^2}{\sigma_U^2}\left(u_0 - \mathrm{sgn}\,(\xi_1)\,\sqrt{|\xi_1|}\right)$$

$$c = a^2\sqrt{\sigma_{\ddot{U}}^2 - \frac{\sigma_{\dot{U}}^4}{\sigma_U^2}} \tag{18}$$

and Φ and ϕ denote the distribution and the density of the standard Gaussian variable. From Eq. 12,

$$E[\dot{\xi}_n(t) \;+/\; \underline{\xi}(t) = \underline{\xi}] = \frac{1}{\sqrt{2a}}\left[c\,\phi\left(\frac{b}{c}\right) + b\,\Phi\left(\frac{b}{c}\right)\right] \tag{19}$$

The mean crossing rate of $\underline{\xi}(t)$ out of the safe domain D is, from Eqs. 11 and 19,

$$\nu(r) = \frac{1}{a}\int_{-\infty}^{\infty}\left[c\,\phi\left(\frac{b}{c}\right) + b\,\Phi\left(\frac{b}{c}\right)\right] f_1(\xi_1)\,f_2(\xi - \xi_1)\,d\xi_1 \tag{20}$$

in which the first order densities f_i of $\xi_i(t)$ are (12,13)

$$f_1(\xi_1) = \frac{1}{2\sigma_U\sqrt{2\pi|\xi_1|}}\,\exp\left\{-\frac{1}{2}\left[\frac{\mathrm{sgn}(\xi_1)\sqrt{|\xi_1|} - u_0}{\sigma_U}\right]^2\right\} \tag{21}$$

and

$$f_2(\xi_2) = \frac{1}{a}\,\phi\left(\frac{\xi_2}{a\sigma_{\dot{U}}}\right) \tag{22}$$

Elementary transformations of Eq. 20 give

$$\nu(r) = \frac{\nu_0}{\beta^2}\int_{-\infty}^{\infty} dw\, \exp\left\{-\frac{1}{2}\left[(w-d)^2 + \left(\frac{\xi^* - \mathrm{sgn}(w)w^2}{\beta}\right)^2\right]\right\} * \tag{23}$$

$$\left\{\beta\delta\sqrt{1-(\beta/\delta)^2}\;\phi(d) + \left[2\,\mathrm{sgn}(w)\,w\left(\xi^* - \mathrm{sgn}(u)u^2\right) - \beta^2(\alpha-w)\right]\Phi(-d)\right\}$$

in which,

$$\alpha = \frac{u_0}{\sigma_U}$$

$$\beta = \frac{a\sigma_{\dot{U}}}{\sigma_U^2}$$

$$\delta = \frac{a\sigma_U}{\sigma_U\sigma_{\dot{U}}}$$

$$\nu_0 = \frac{1}{2\pi}\,\frac{\sigma_U}{\sigma_{\dot{U}}}$$

$$d = \frac{2\,\mathrm{sgn}(w)w\left(\xi^* - \mathrm{sgn}(w)w^2\right) - \beta^2(\alpha-w)}{\beta\delta\sqrt{1-(\beta/\delta)^2}}$$

$$\xi^* = \xi/\sigma_U^2$$

$$\tilde{\xi} = \left(\xi^* - \theta\right) / \sqrt{\zeta^2 + \beta^2}$$

$$\theta = E[\xi_1(t)] / \sigma_U^2$$

$$\xi^2 = \mathrm{Var}[\xi_1(t)]/\sigma_U^4$$

The parameters θ and ζ^2 denote scaled values of the mean and variance of the drag process $\xi_1(t)$ and can be obtained in closed form from the density in Eq. 21 (12,13).

As previously mentioned, the mean outcrossing rate in Eq. 20 coincides with the mean upcrossing rate of level $r = a_1\xi/k$ of the response process R(t) in Eq. 8. This mean upcrossing rate depends on the joint density of R(t) and $\dot{R}(t)$ and can be obtained from this density and Rice's formula (8,19). The mean outcrossing rate has also been approximated from the "point-crossing formula". According to this formula, the mean upcrossing rate of a sum of two processes, such as the drag and inertia processes in Eq. 8, can be approximated by (12,13,15)

$$\nu^{p.c.}(r) = \int \nu_1(\xi - \xi_2)\, f_2(\xi_2)\, d\xi_2 + \int \nu_2(\xi - \xi_1)\, f_1(\xi_1) d\xi_1 \qquad (25)$$

in which $\nu_i(u)$, $i = 1,2$, denotes the mean upcrossing rate of level u of $\xi_i(t)$. The mean outcrossing rate ν has also been approximated from linearized representations of the response, e.g., for $u_0 > 0$,

$$R_L(t) = \frac{1}{k}\left[a_1\left(u_0^2 + 2u_0\, U(t)\right) + a_2\, \dot{U}(t)\right] \qquad (26)$$

Note that the mean upcrossing rate of the linearized response, ν^L, can be obtained simply because $R_L(t)$ is a Gaussian process (12,13).

Figure 2 shows with solid and dotted lines ratios of the mean crossing rates ν/ν^L and $\nu^{p.c.}/\nu^L$ for the power spectral density in Eq. 2 with $\omega_p = 0.8$ rad/sec., $\bar{\omega} = 3\omega_p = 2.4$ rad/sec., wind speed v = 50 ft/sec., and zero, intermediate, and large current ($\alpha = 0.0$, 0.5, and 1.0). The parameter β (Eq. 23) is related to the relative importance of inertia and drag forces. Large values of β correspond to inertia dominated wave forces while small values of this parameter are typical to drag dominated wave forces. For the wave forces

in this figure $\beta = 1.09$ d. The ratios of mean crossing rates show that the linear approximation can underestimate significantly the peak response. Note that the point crossing formula constitutes a satisfactory approximation of ν. The standardized threshold in this figure is measured in standard deviation units from the mean and is based on exact values of the mean and the standard deviation of the response.

Figure 3 shows standardized dimensionless averages of the peak response during storms of various durations τ for a wind speed of 70 ft/sec and zero current. These averages are based on Eqs. 9 and 23 and an approximation of the largest distribution of the response in Ref. 24. From this reference,

$$F_\tau(r) \approx \left[\bar{F}(r)\right]^{n_\tau} \tag{27}$$

in which $\bar{F}$ = the distribution of individual response peaks and n_τ = the average number of such peaks in τ. $\bar{F}(r)$ can be obtained from the fraction of individual peaks which do not exceed r. Note that the approximations shown in this figure are in good agreement.

DYNAMIC RESPONSE

Consider a simple oscillator with mass m, damping c, and stiffness k subject to the wave force process $W(t) = X(t)$ or $Y(t)$ in Eq. 3 or 6. The displacement of the oscillator, R(t), satisfies the differential equation

$$m\,\ddot{R}(t) + c\dot{R}(t) + k\,R(t) = W(t) \tag{28}$$

and is generally a non-Gaussian random process which has stationary characteristics during the steady-state period of oscillations. Denote by $\omega_0 = \sqrt{k/m}$ and $\zeta = c/(2m\,\omega_0)$ the natural frequency and the damping ratio of the

oscillator. It is assumed in the analysis that $\zeta = 5\%$.

This section develops probabilistic characteristics of the steady-state response R(t) "exactly" by simulation and approximately by statistical linearzation and time-discretization of the wave force process. The approximate results are evaluated by simulation.

Simulation Method

Figure 4 shows a discrete approximation of the power spectral density in Eq. 2. According to this approximation, U(t) has power at N frequencies ω_i which can be measured by the variances σ_i^2. The process can be represented by

$$U(t) = \sum_{i=1}^{N} \left(A_i \cos \omega_i t + B_i \sin \omega_i t\right) \tag{29}$$

in which A_i and B_i are zero-mean, mutually independent Gaussian variables (3,21). The variance of A_i and B_i is σ_i^2. From Eq. 29, the wave particle acceleration has the expression

$$\dot{U}(t) = \sum_{i=1}^{N} \omega_i \left(- A_i \sin \omega_i t + B_i \cos \omega_i t\right) \tag{30}$$

The simulation method involves three phases. First, realizations of U(t) and $\dot{U}(t)$ are generated for storm of any duration τ from Eqs. 29 and 30 and samples of $\{A_i, B_i\}$, i =1, ..., N. These realizations and Eqs. 3, 6, or 7 provide samples of the wave force process. Second, deterministic dynamic analyses are performed to determine the response in $(0,\tau)$ to these samples. The analyses involve time-domain integrations and determinations of the peak response in τ, the rate of upcrossings relative to various thresholds, and other response descriptors for every sample of the wave force process. Third,

the sample descriptors are employed to calculate means and variances of the response, the average peak response in τ, and mean upcrossing rates.

Statistical Linearization Method

The method was applied extensively to the solution of complex dynamic problems, particularly for the estimation of the second-moment descriptors of the response, e.g., the mean and variance (22,23). Recently, the method was employed to find the mean and variance of the response of offshore structures to wave forces characterized by the interactive form of the Morison's equation in Eq. 6 (23).

According to the statistical linearization method, the solution of a non-linear differential equation can be approximated by the solution of a linear differential equation that can be obtained by minimizing an expected error. Thus, the response of the structural model in Eq. 28 with $W(t) = Y(t)$ in Eq. 6 can be approximated by the solution of a linear differential equation excited by linear functions of $U^*(t)$. Since these functions are Gaussian processes, the response is itself a Gaussian process. However, the actual distribution of the response can differ significantly from the Gaussian distribution.

Figure 5 shows ratios ν/ν^L of exact to approximate mean upcrossing rates of the response R(t) in Eq. 28 to the interactive wave force Y(t) in Eq. 6 with $c_m = 2.0$, $c_d = 1.0$, d = 0.5 ft., and the power spectral density in Eq. 2 for $\bar{\omega} \simeq 15$ rad/sec. and v = 50 ft/sec. The exact and approximate mean upcrossing rates were obtained by the simulation method in the previous section and by statistical linearization. The simulation method involves N = 1024 frequencies and time-domain integrations with a time step $\Delta t = 0.2$ sec. Note that the differences between the mean upcrossing rates ν and ν^L increase with the threshold and can be significant for relatively large values of the threshold. From Eq. 9, the disribution $\exp(-\nu_L \tau)$ of the peak response based on the approximate mean crossing rate ν_L is generally inaccurate and its use results in

unconservative estimates of the average peak response. Thus, the statistical linearization method should not be applied to estimate the peak response. A possible use of the method could be in fatigue studies involving exceedings of relatively low thresholds. For such thresholds, the exact and approximate mean upcrossing rates do not differ significantly. The large errors in statistical linearization are primarily caused by the implicit assumption in this method that the response is a Gaussian process. The assumption is particularly erroneous for large thresholds and small currents due to differences between the Gaussian distribution and the actual distribution of response.

Time-Discretization Method

Assume that W(t) in Eq. 28 is equal to the wave force X(t) in Eq. 3. Let $\{X_k\}$ be a series with time step Δ and the same marginal distribution as X(t) which takes on constant and independent values within the holding periods Δ.

From Eq. 28, the response to X(t) is

$$R(t) = \int_0^t h(t-\tau)\, X(\tau)\, d\tau \tag{31}$$

when the oscillator is at rest at t = 0. If X(t) is approximated by the series $\{X_k\}$, the response and its derivative have the expressions

$$R(t) = \sum_{k=1}^{n} h_k\, X_k \tag{32}$$

and

$$\dot{R}(t) = \sum_{k=1}^{n} \dot{h}_k\, X_k \tag{33}$$

at any $t = n\Delta$, in which

$$h_k = \int_{(k-1)\Delta}^{k\Delta} h(t-\tau)\, d\tau \tag{34}$$

and $\dot{h}_k = dh_k/dt$. For the simple oscillator in Eq. 28,

$$h_k = \frac{e^{-\zeta\alpha_0(n-k)}}{\omega_1\omega_0} \{\zeta \sin((n-k)\alpha_1) + \sqrt{1-\zeta^2} \cos((n-k)\alpha_1) - e^{-\zeta\alpha_0} [\zeta \sin((n-k+1)\alpha) + \sqrt{1-\zeta^2} \cos((n-k+1)\alpha)]\} \tag{35}$$

and

$$\dot{h}_k = \frac{1}{\omega_1} [e^{-\zeta\alpha_0(n-k+1)} \sin((n-k+1)\alpha_1) - e^{-\zeta\alpha_0(n-k)} \sin((n-k)\alpha_1)] \tag{36}$$

in which $\omega_0 = \sqrt{k/m}$, $\zeta = c/(2\,\omega_0 m)$, $\omega_1 = \omega_0\sqrt{1-\zeta^2}$, $\alpha_0 = \omega_0\Delta$, and $\alpha_1 = \omega_1\Delta$.

From Eqs. 32 to 36, one can determine moments of the response vector $\{R(t), \dot{R}(t)\}$. For example, the covariance matrix of this vector has the components

$$\begin{aligned} \sigma^2 &= \sigma_X^2 \sum_{k,\ell=1}^{n} \rho_{k\ell}\, h_k\, h_\ell \\ \dot{\sigma}^2 &= \sigma_X^2 \sum_{k,\ell=1}^{n} \rho_{k\ell}\, \dot{h}_k\, \dot{h}_\ell \\ \mathrm{Cor}(R,\dot{R}) &= \sigma_X^2 \sum_{k,\ell=1}^{n} \rho_{k\ell}\, h_k\, \dot{h}_\ell \end{aligned} \tag{37}$$

if $\{X_k\}$ were a correlated series with variance σ_X^2 and correlation coefficient

$\rho_{k\ell}$ between X_k and X_ℓ. These equations simplify significantly for independent excitations, as considered here, because $\rho_{k\ell}$ is one for $k=\ell$ and zero other wise. In this case (10),

$$\sigma^2 = \frac{\Delta}{4\zeta\omega_0{}^2}\,\sigma_X^2 \tag{38}$$

From Eq. 32, the characteristic function of the response is

$$\psi_n(u;\, h_1,\, \ldots,\, h_n) = \prod_{k=1}^{n} \psi(uh_k) \tag{39}$$

in which ψ = the characteristic function of the random variable X(t). ψ_n can be inverted by Fast Fourier Transform to determine the density, f, and the distribution, F, of R(t). The characteristic function ψ of X(t) is equal to the product of the characteristic functions ψ_1 and ψ_2 of the drag force $a_1X_1(t)$ and inertia force $a_2X_2(t)$ because these forces are independent at any time t. These characteristic functions are

$$\psi_1(u) = \frac{1}{2\sqrt{2}}\left\{\frac{1}{\sqrt{s_1}}\,\exp\left(\frac{\alpha^2 - 2\alpha s_1}{4\,s_1}\right)\operatorname{erfc}\left(\frac{\alpha}{2\sqrt{s_1}}\right) + \right.$$

$$\left. + \frac{1}{\sqrt{s_2}}\,\exp\left(\frac{\alpha^2 - 2\alpha s_2}{4s_2}\right)\operatorname{erfc}\left(-\frac{\alpha}{2\sqrt{s_2}}\right)\right\} \tag{40}$$

in which $s_1 = \frac{1}{2}\left(1 + 2\sqrt{-1}\ ua_1\sigma_u{}^2\right)$, $s_2 = \frac{1}{2}\left(1 - 2\sqrt{-1}\ ua_1\sigma_u{}^2\right)$, $\operatorname{erfc}\left(-\sqrt{-1}\ z\right) = 1 + \frac{2\sqrt{-1}}{\sqrt{\pi}}\int_0^z e^{t^2}\,dt$, and

$$\Psi_2(u) = \exp\left(-\frac{1}{2} a_2^2 \sigma_{\dot{U}}^2 u^2\right) \tag{41}$$

Two approximations are considered for the mean upcrossing rate of level r of R(t), $\nu(r)$. First, it is assumed that R(t) and the translation process

$$R_T(t) = F^{-1}\left(\Phi(\zeta(t))\right) \tag{42}$$

have the same crossing characteristics. The process $\zeta(t)$ in this equation is a stationary Gaussian process with zero-mean and unit variance (11). The variance of $\dot{\zeta}(t) = d\zeta(t)/dt$ is

$$\sigma_{\dot{\zeta}}^2 = \dot{\sigma}^2 \frac{1}{\int_{-\infty}^{\infty} \frac{\phi^3(z)\, dz}{\{f[F^{-1}(\Phi(z))]\}^2}} \tag{43}$$

According to this approximation (10),

$$\nu(r) \simeq \frac{\sigma_{\dot{\zeta}}}{\sqrt{2\pi}} \phi\left(\Phi^{-1}(F(r))\right) \tag{44}$$

Second, it is assumed that $\dot{R}(t)$ is independent of R(t) and follows a Gaussian distribution (11). The assumption results in the approximation

$$\nu(r) \simeq \frac{\dot{\sigma}}{\sqrt{2\pi}} f(r) \tag{45}$$

Figure 6 shows "exact" mean upcrossing rates of R(t) and approximations of these mean rates in Eq. 44 for wave forces with $c_m = 2.0$, $c_d = 1.0$, and $d = 0.5$ ft. It was found that the estimates in Eq. 44 improve significantly if the

time step Δ of the independent series $\{X_k\}$ is determined from the condition that the variance σ^2 in Eq. 38 matches the actual variance of the response, corresponding to the continuous wave force process X(t). This variance can be obtained simply and accurately from Eq. 37 if the time step $\Delta = \Delta^*$ is small (e.g, a tenth of the period of the oscillator) and $\rho_{k\ell}$ are the correlation coefficients of lag $|k-\ell|\Delta^*$ of X(t). These correlations are (4)

$$\rho_{k\ell} = B_X\left((k-\ell)\Delta^*\right) \;/\; B_X(0) \tag{46}$$

in which

$$B_X(\tau) = a_1^2\,\sigma_U^4\, g(\alpha,\,\alpha,\,\rho_U(\tau)) + a_2^2\,\sigma_{\dot U}^2\,\rho_{\dot U}(\tau) - \\ - 4a_1^2\,\sigma_U^4\left[\alpha\,\phi(\alpha) + (1+\alpha^2)\left(\Phi(\alpha) - \frac{1}{2}\right)\right]^2 \tag{47}$$

$$g(\alpha,\,\alpha,\,s) = \left[(1+\alpha^2)^2 + 4\alpha^2 s + 2s^2\right]\left[1-4\,\Phi(-\alpha) + 4\,\Phi(\alpha,\,\alpha,\,s)\right] \\ + \frac{2}{\pi}\left(1-s^2\right)^{1/2}(\alpha^2+3s)\exp\left(-\frac{\alpha^2}{1+s}\right) + \\ + 2\left(\frac{2}{\pi}\right)^{1/2}\left[\alpha(1+\alpha^2) + 4\,\alpha s\right]\exp\left(-\frac{\alpha^2}{2}\right)\left[\Phi\left(\alpha(1-s)\right) - \frac{1}{2}\right] \tag{48}$$

ρ_U and $\rho_{\dot U}$ = the normalized covariance functions of U(t) and $\dot U$(t), and $\phi(\cdot,\cdot;\cdot)$ = the bivariate normal distribution.

From Fig. 6 developed for structures with 5% damping ratios, the time-discretization method is simple and provides satisfactory approximations for the mean upcrossing rates of the response. The method was also applied successfully to the analysis of structures with much larger damping ratios. Such damping characteristics may be used to model effects of flow-structure interaction

(2,9). A limitation of the method is that it becomes inefficient computationally when applied to analyze structures with large periods of vibration.

CONCLUSIONS

Mean upcrossing rates and other probabilistic descriptors were developed for the quasi-static and dynamic response of offshore platforms subject to wave forces. The descriptors are exact for quasi-static responses and approximate for dynamic responses.

Results show that the approximate mean crossing rates of the response obtained by the statistical linearization method are generally inaccurate and on the unconservative side for both quasi-static and dynamic structural responses. The use of the method in the dynamic analysis of offshore platforms can result in unsafe designs. On the other hand, the peak of the dynamic response of offshore platforms can be approximated satisfactorily by a method proposed in this paper which involve serial representations of the wave force process.

REFERENCES

1. American Petroleum Institute Recommended Practice for Planning, Designing and Construction of Fixed Offshore Platforms, American Petroleum Institute, API RP 2A, Ninth Edition, Washington, D.C., November 1977.

2. Anagnostopoulos, S. A., "Dynamic Response of Offshore Platforms to Extreme Waves Including Fluid-Structure Interaction," Engineering Structures, Vol. 4, July, 1982, pp. 179-185.

3. Borgman, L. E., "Ocean Wave Simulation for Engineering Design," Journal of Waterways and Harbors Division, ASCE, Vol. 95, No. WW4, November, 1969, pp. 557-583.

4. Borgman, L. E., "Random Hydrodynamic Forces on Objects," Annals of Mathematical Statistics, Vol. 38, 1967, pp. 37-51.

5. Borgman, L. E., "Statistical Models for Ocean Waves and Wave Forces," Advances in Hydroscience, Vol. 8, 1972, pp. 139-181.

6. Burrows, R., "Probabilistic Description of the Response of Offshore Structures to Random Loading," Mechanics of Wave-Induced Forces on Cylinders, T. L. Shaw, ed., Pitman Advanced Publishing Program, San Francisco, CA, 1979, pp. 577-595.

7. Burrows, R., "Quasistatic Response of Offshore Structures Using Probabilistic Methods," Applied Mathematical Modelling, Vol. 1, Sept. 1977, pp. 325-332.

8. Cramer, H. and Leadbetter, M. R., Stationary and Related Stochastic Processes, John Wiley & Sons, New York, 1967.

9. Fish, P. R., Dean, R. B., and Heaf, N. J., "Fluid-Structure Interaction in Morison's Equation for the Design of Offshore Structures," Engineering Structures, Vol. 2, Jan. 1980, pg. 15-26.

10. Grigoriu, M., "Dynamic Response of Offshore Platforms to Environmental Loads," Proceedings of the 4th ASCE Specialty Conference on Probabilistic Mechanics and Structural Reliability, American Society of Civil Engineers, January, 1984, pp. 115-118.

11. Grigoriu, M., "Crossings of Non-Gaussian Translation Processes," Journal of Engineering Mechanics, ASCE, Vol. 110, No. EM4, April 1984, pp. 610-620.

12. Grigoriu, M., and Alibe, B., "Practical Approximations of Peak Wave Forces," Research Report NBS-GCR-84-481, National Bureau of Standards, November 1984.

13. Grigoriu, M., "Extremes of Wave Forces," Journal of Engineering Mechanics Division, ASCE, Vol. 110, No. 12, December 1984, pp. 1731-1742.

14. Hallam, M.G., Heaf, N. J., and Wootton, L. R., Dynamics of Marine Structures: Methods of Calculating the Dynamic Response of Fixed Structures Subject to Wave and Current Action, CIRIA Under Water Engineering Group, Report UR8, London, October, 1978.

15. Larrabee, R. D., and Cornell, C. A., "Combination of Various Load Processes," Journal of the Structural Division, ASCE, Vol. 107, No. ST1, Proc. Paper 15999, Jan., 1981, pp. 223-239.

16. Moe, G., "Long-Term Wave-Force Statistics for a Vertical Pile," Coastal Engineering, Vol. 2, 1979, pp. 297-311.

17. Moe, G., and Verley, R. L. P., "Hydrodynamic Damping of Offshore Structures in Waves and Currents," Proceedings of the Offshore Technology Conference, paper No. 3798, 1980, pp. 37-44.

18. Morison, J. R., O'Brien, M. P., Johnson, J. W., and Scahff, S. A., "The Force Exerted by Surface Waves on Piles," Petroleum Transactions, American Institute of Mining Engineers, Vol. 189, 1950, pp. 149-154.

19. Naess, A., "Prediction of Extremes of Morison-type Loading. An Example of General Methods,: Ocean Engineering, Vol. 10, No. 5, 1983, pp. 313-324.

20. Sarpkaya, T., and Isaacson, M., Mechanics of Wave Forces on Offshore Structures, Van Nostrand Reinhold Company, New York, 1981.

21. Shinozuka, M., "Monte Carlo Solution of Structural Dynamics," Computers and Structures, Vol. 2, 1972, pp. 855-873.

22. Soong, T. T., Random Differential Equations in Science and Engineering, Academic Press, New York, 1973.

23. Spanos, P-T. D., and Chen, T. W., "Random Response to Flow-Induced Forces," Journal of Engineering Mechanics, ASCE, Vol. 107, No. 6, Dec. 1981, pp. 1173-1190.

24. Tickell, R. G., "Continuous Random Wave Loading on Structural Members," The Structural Engineer, Vol. 55, No. 5, May 1977, pp. 209-222.

25. Tung, C. C., "Peak Distribution of Random Wave-Current Force," Journal of the Engineering Mechanics Division, ASCE, Vol. 100, No. EM5, Proc. Paper 10843, Oct., 1976, pp. 873-884.

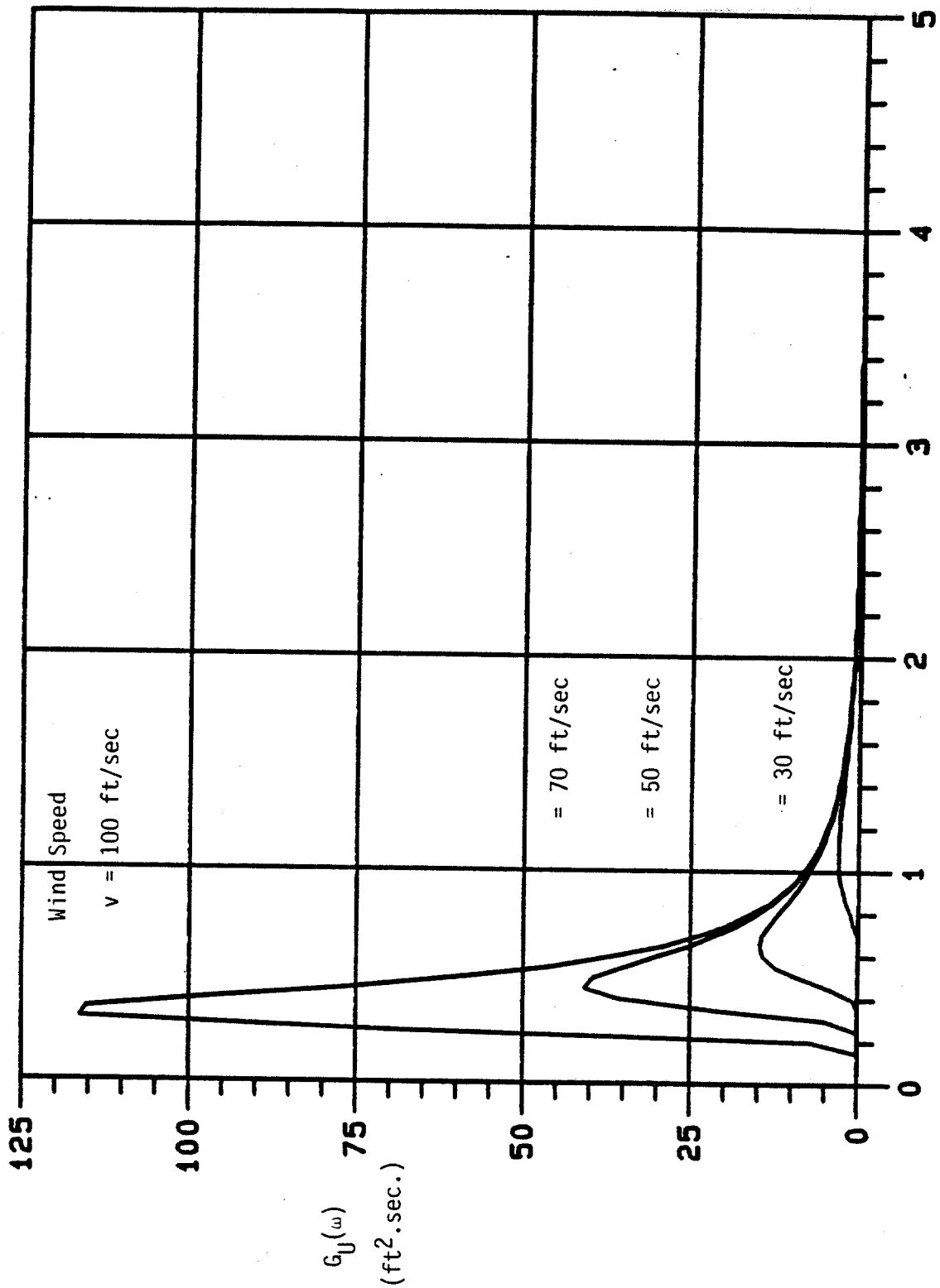

Figure 1. Mean Power Spectral Density of Wave Particle Velocity.

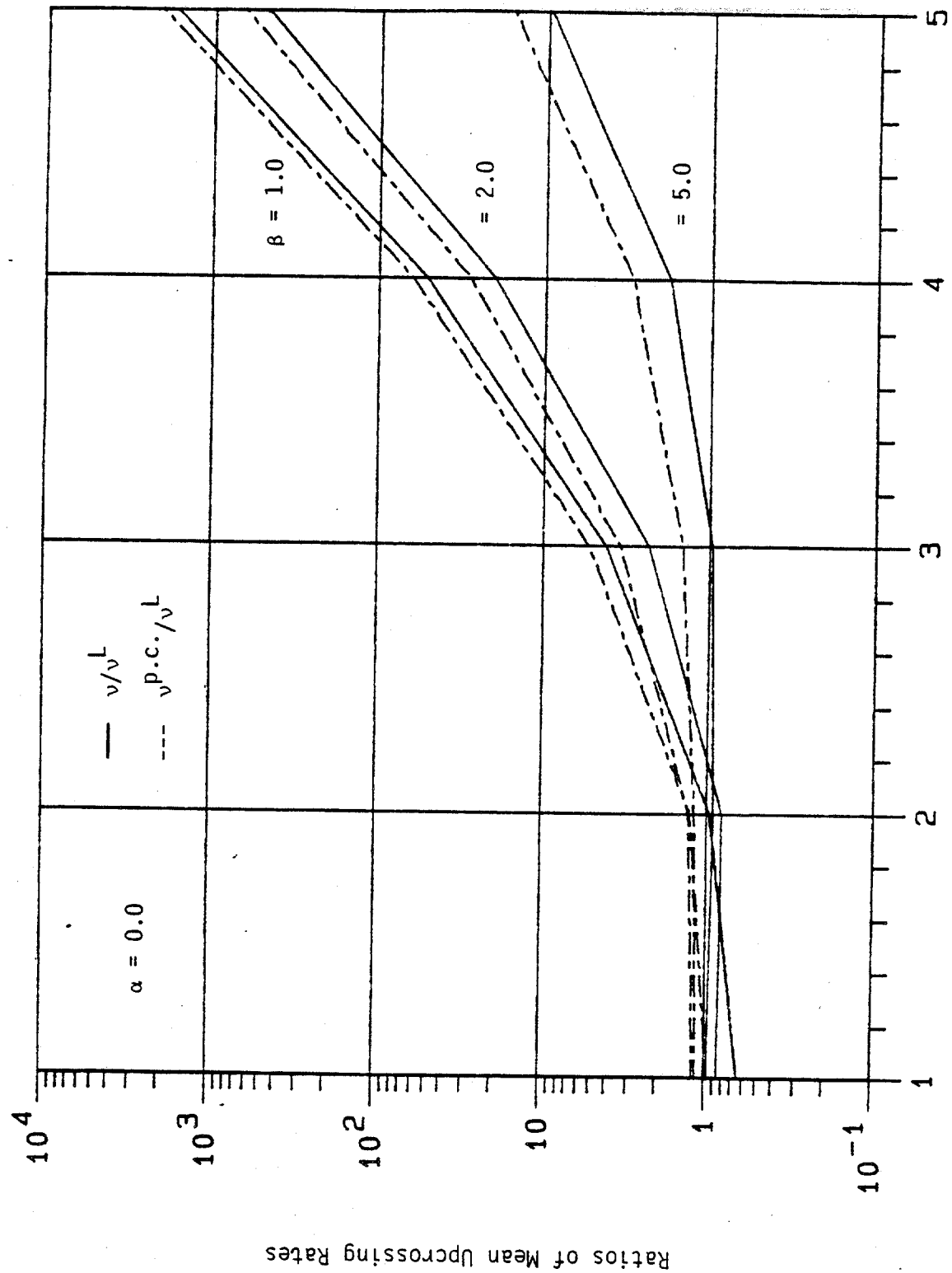

Figure 2(a). Ratios of Mean Upcrossing Rates of Quasi-Static Responses.

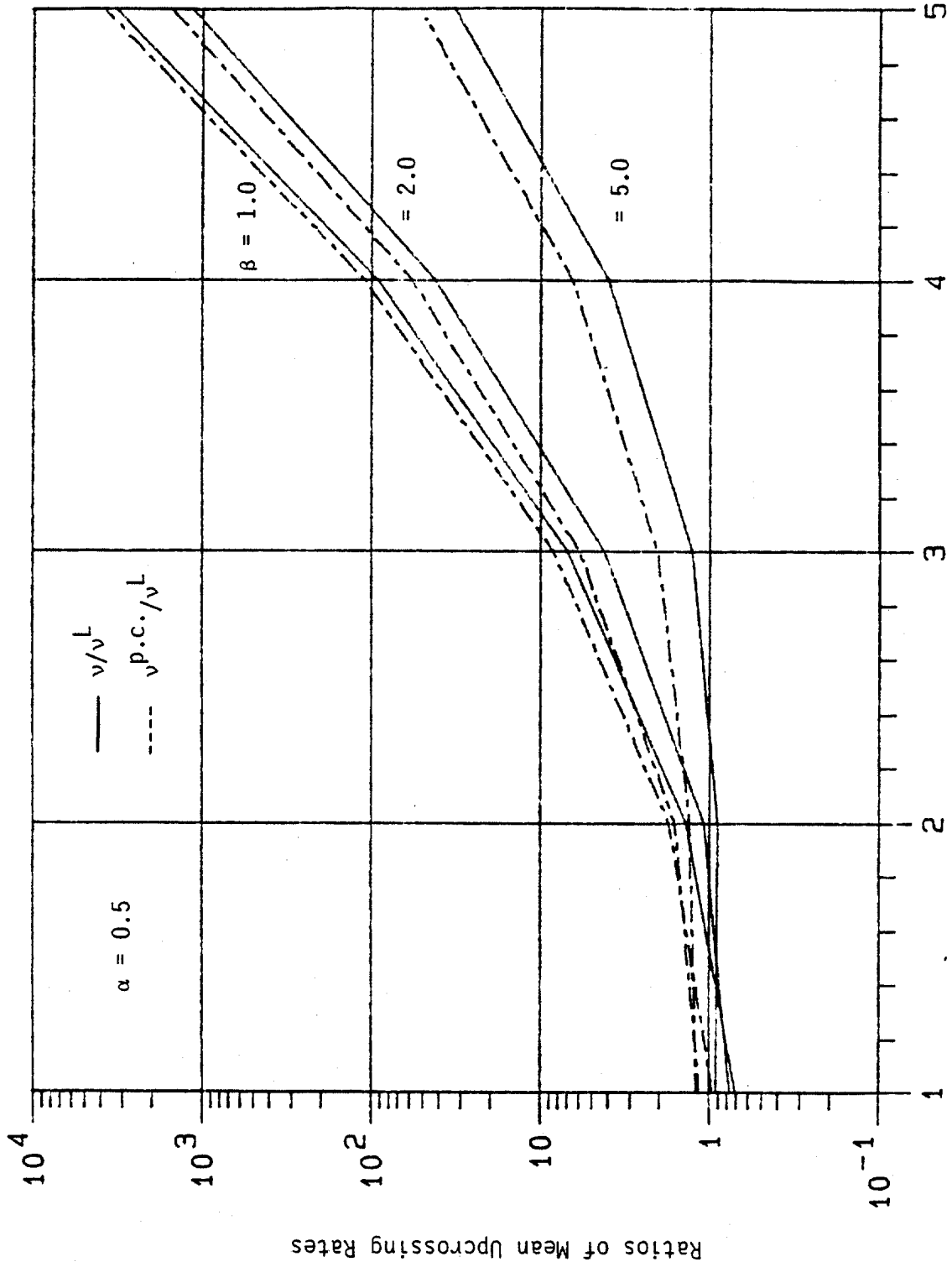

Figure 2(b). Ratios of Mean Upcrossing Rates of Quasi-Static Responses.

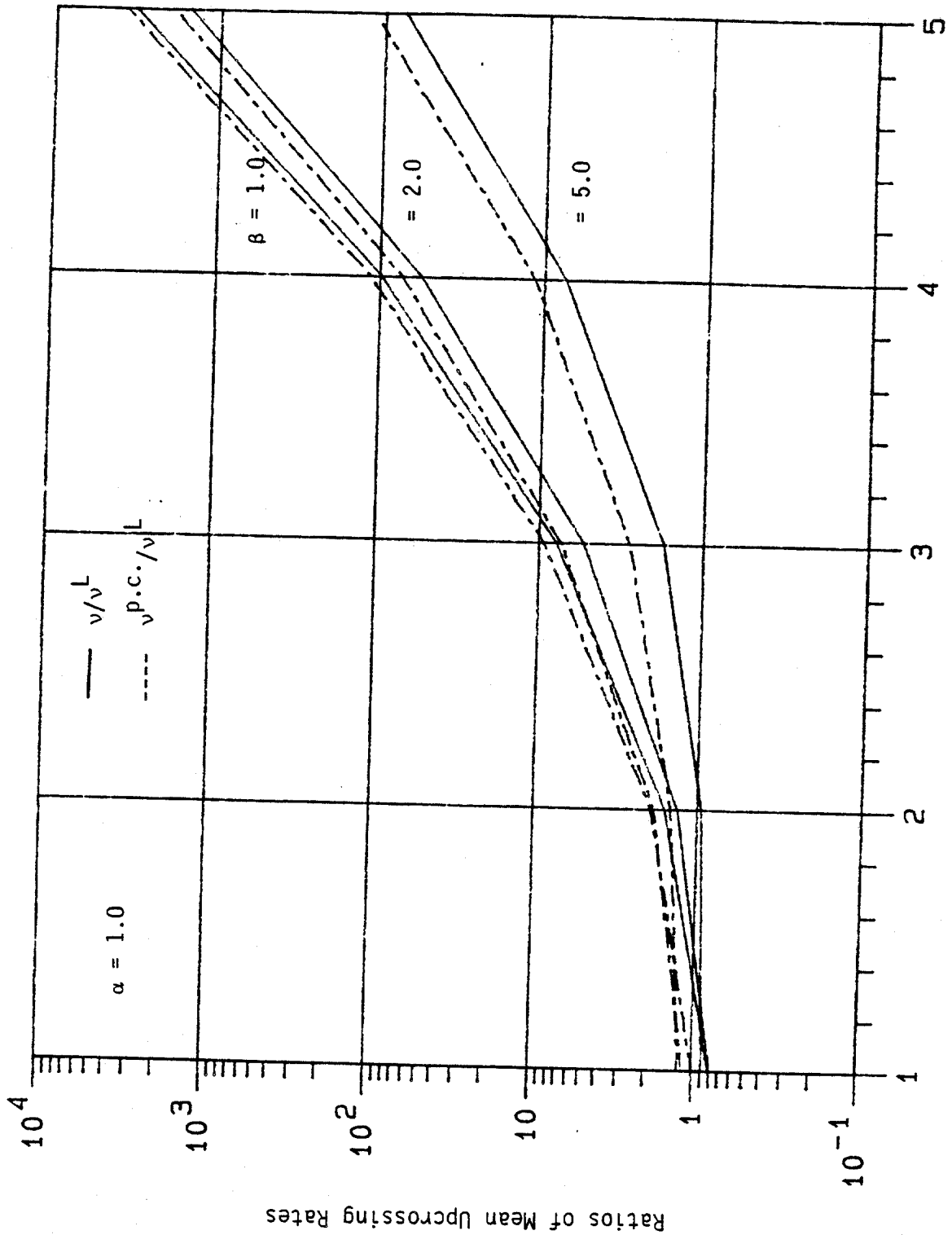

Figure 2(c). Ratios of Mean Upcrossing Rates of Quasi-Static Responses

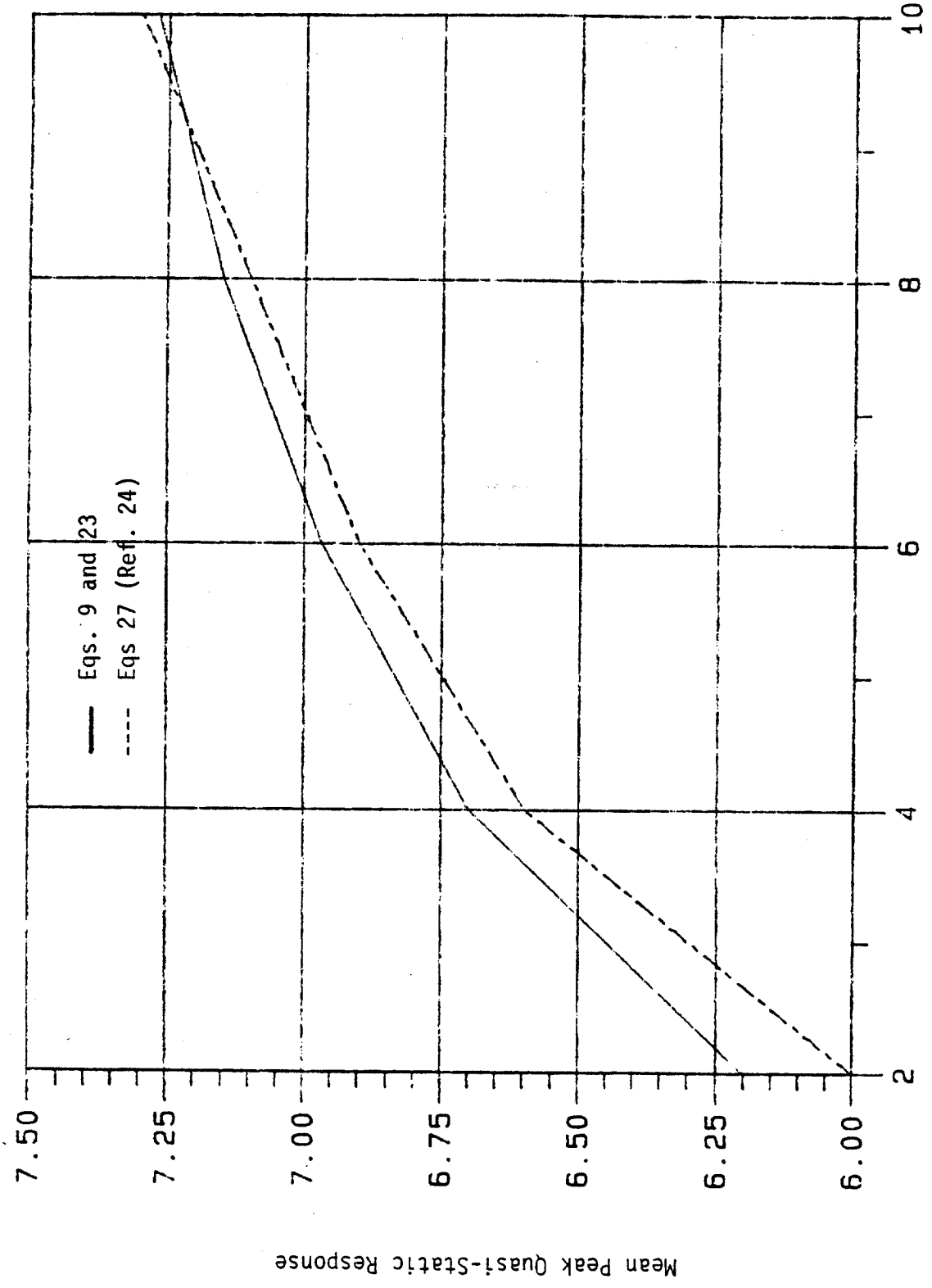

Figure 3. Averages of Peak Quasi-Static Response.

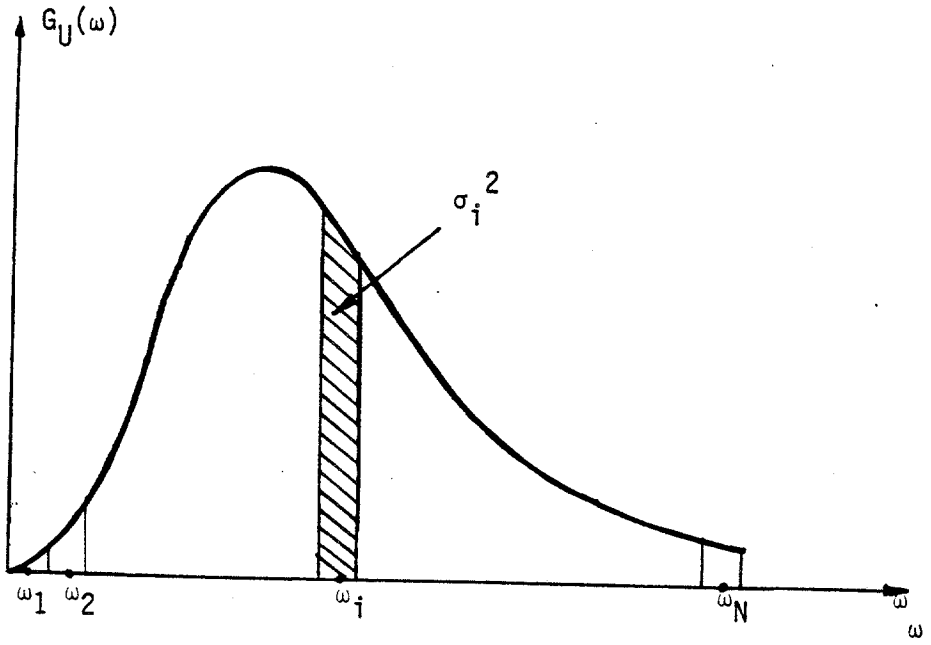

Figure 4. Discrete Approximation of Mean Power Spectral Density.

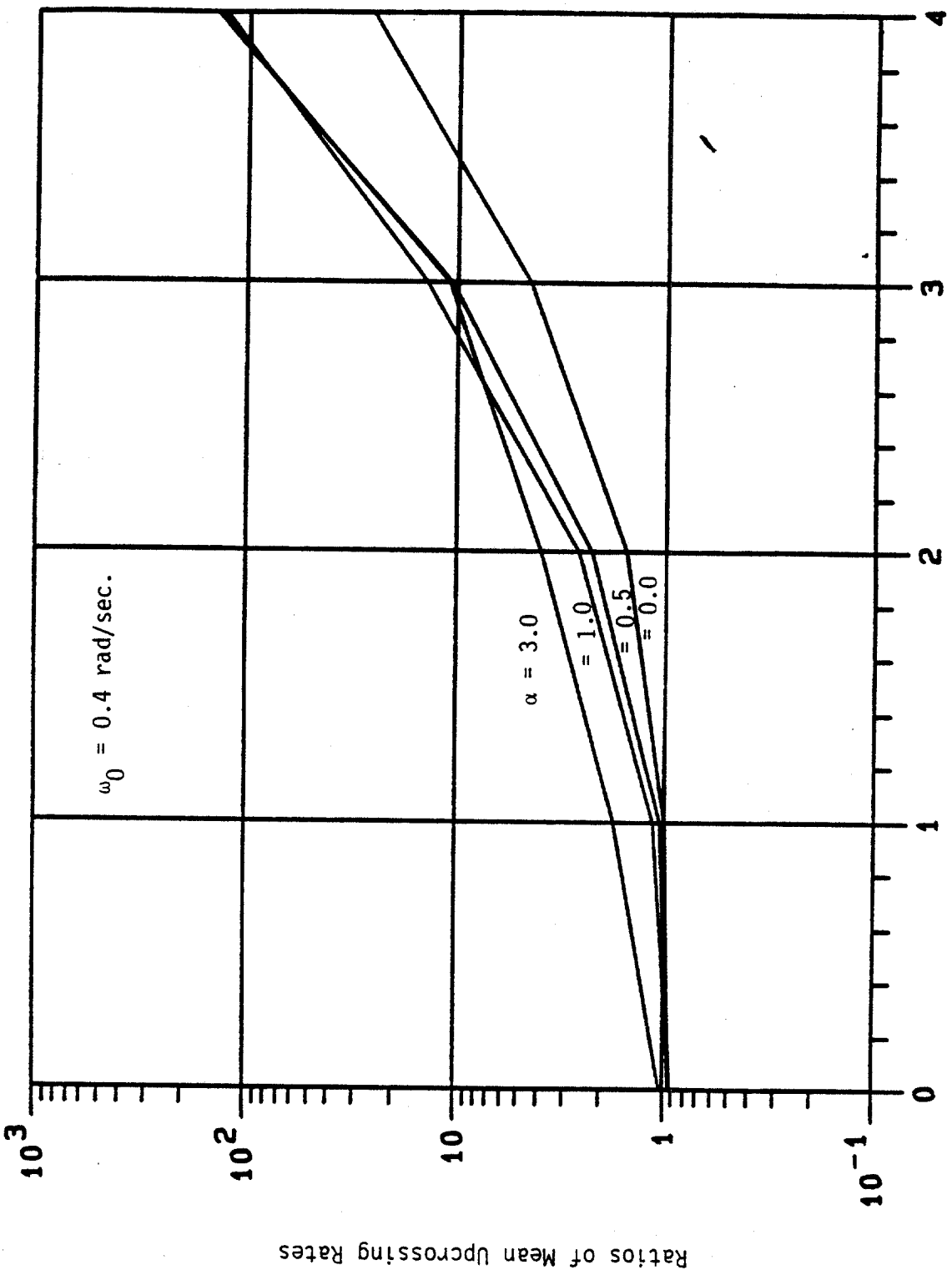

Figure 5(a). Ratios of Exact to Approximate (Statistical Linearization Method) Mean Upcrossing Rates of Dynamic Responses.

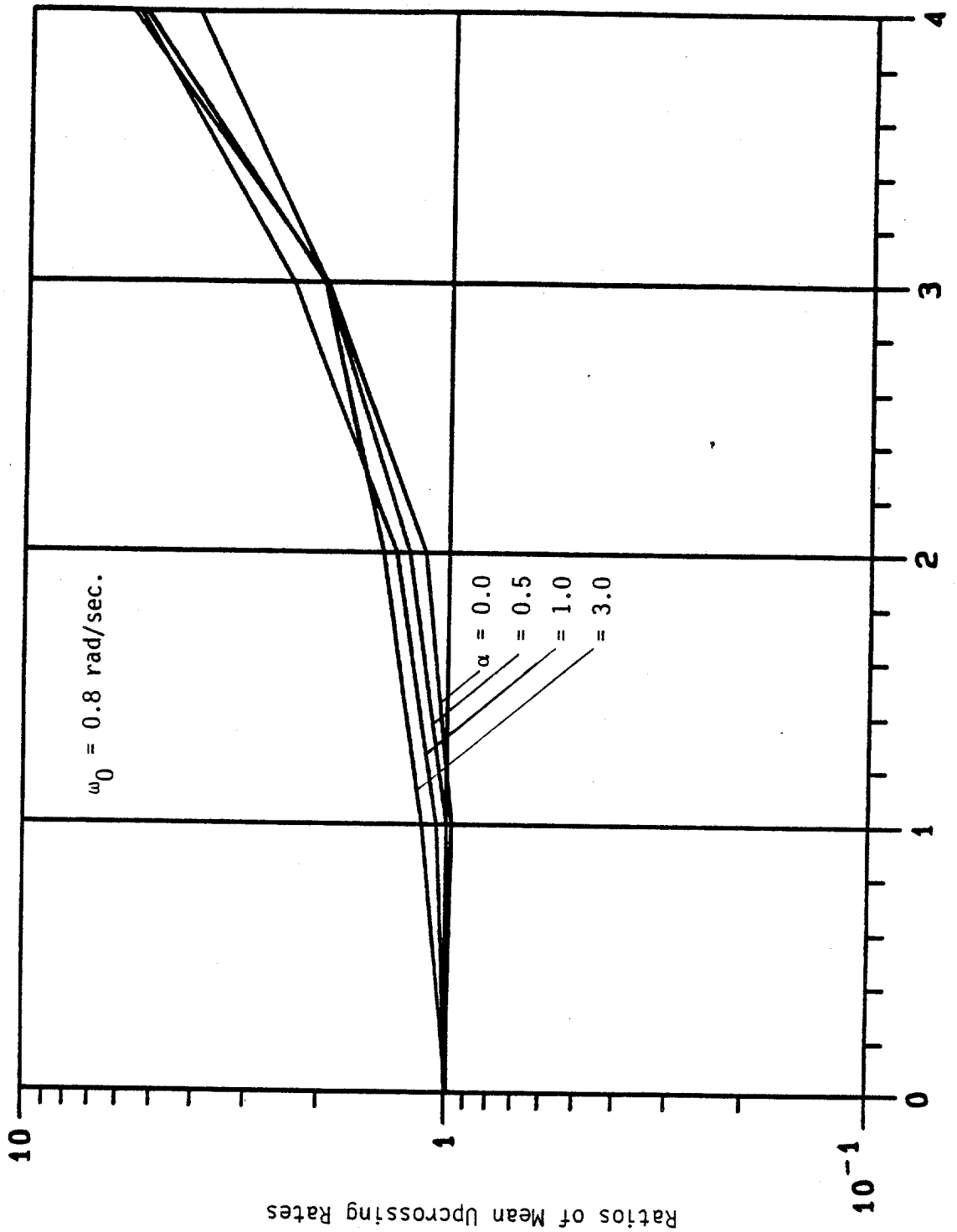

Figure 5(b). Ratios of Exact to Approximate (Statistical Linearization Method) Mean Upcrossing Rates

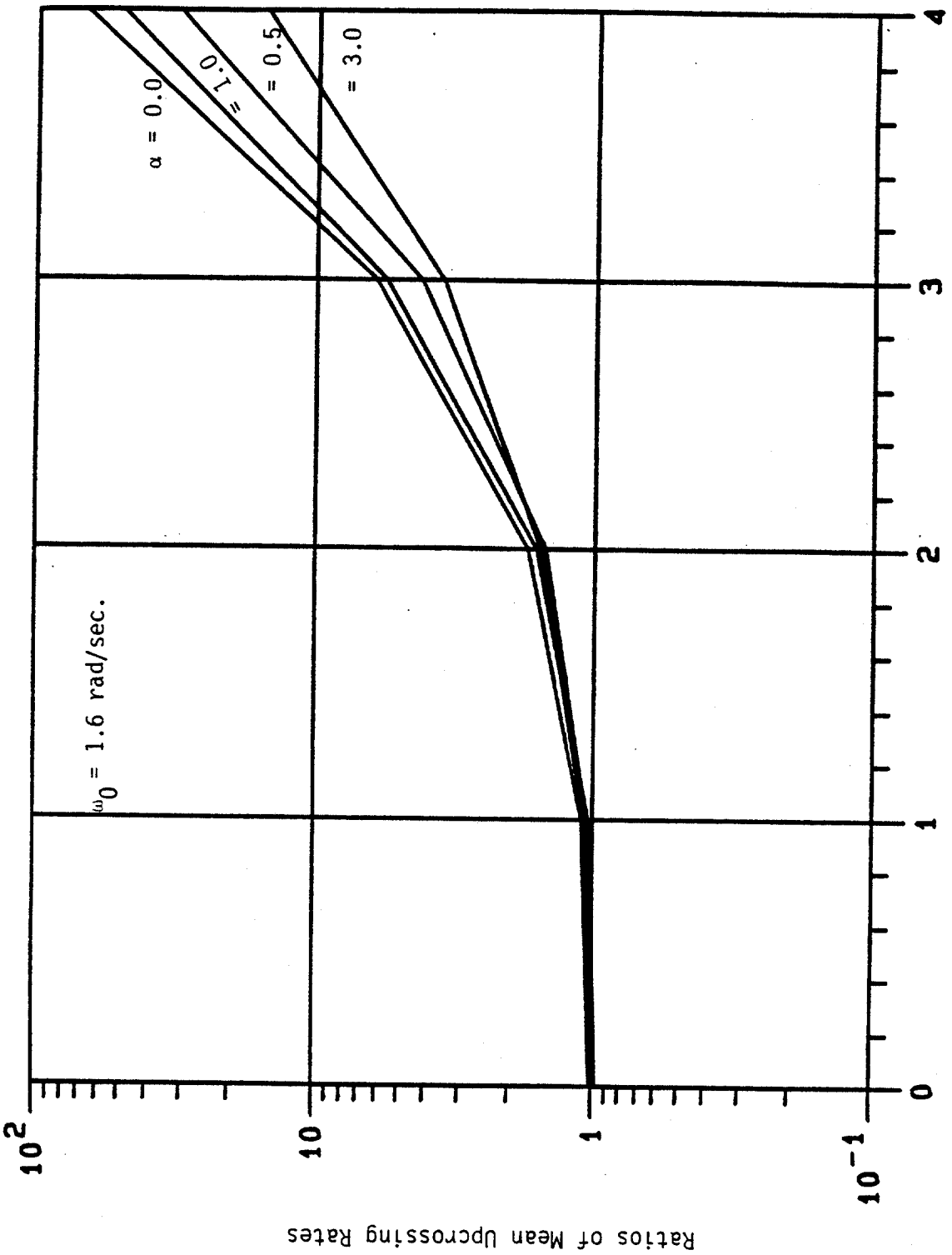

Figure 5(c). Ratios of Exact to Approximate (Statistical Linearization Method) Mean Upcrossing Rates of Dynamic Responses.

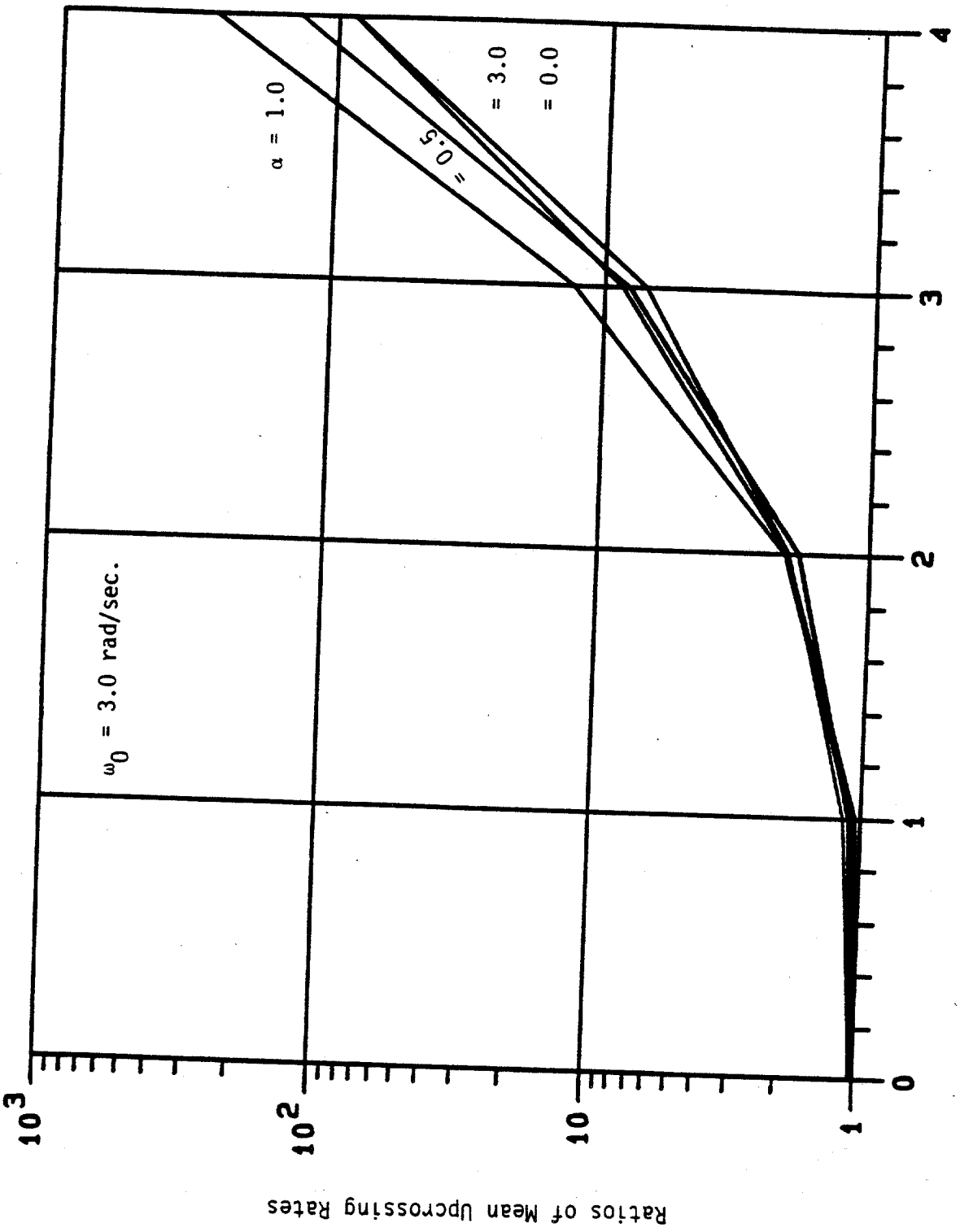

Figure 5(d). Ratios of Exact to Approximate (Statistical Linearization Method) Mean Upcrossing Rates

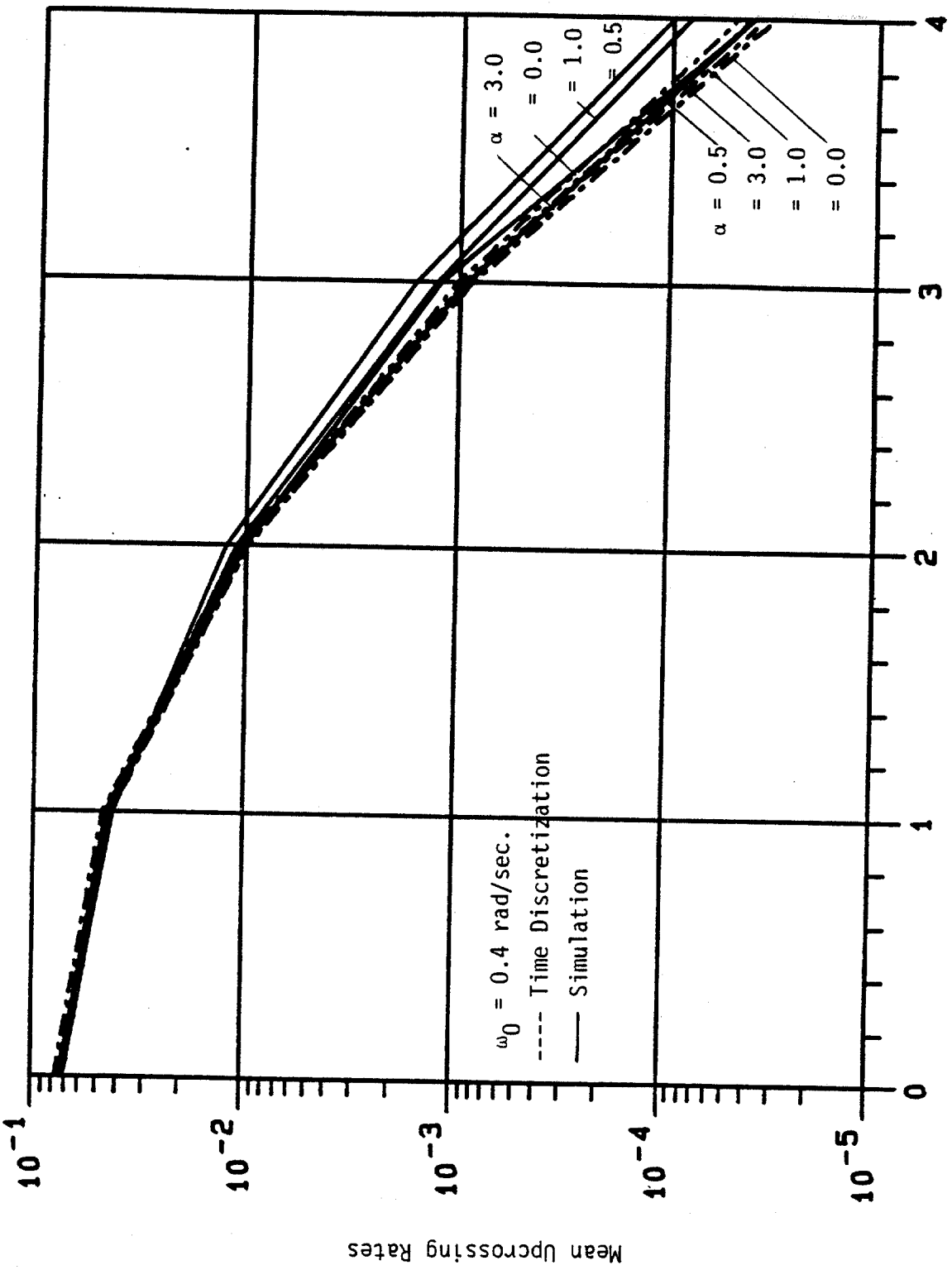

Figure 6(a). Exact and Approximate (Time-Discretization Method) Upcrossing Rates of Dynamic Response.

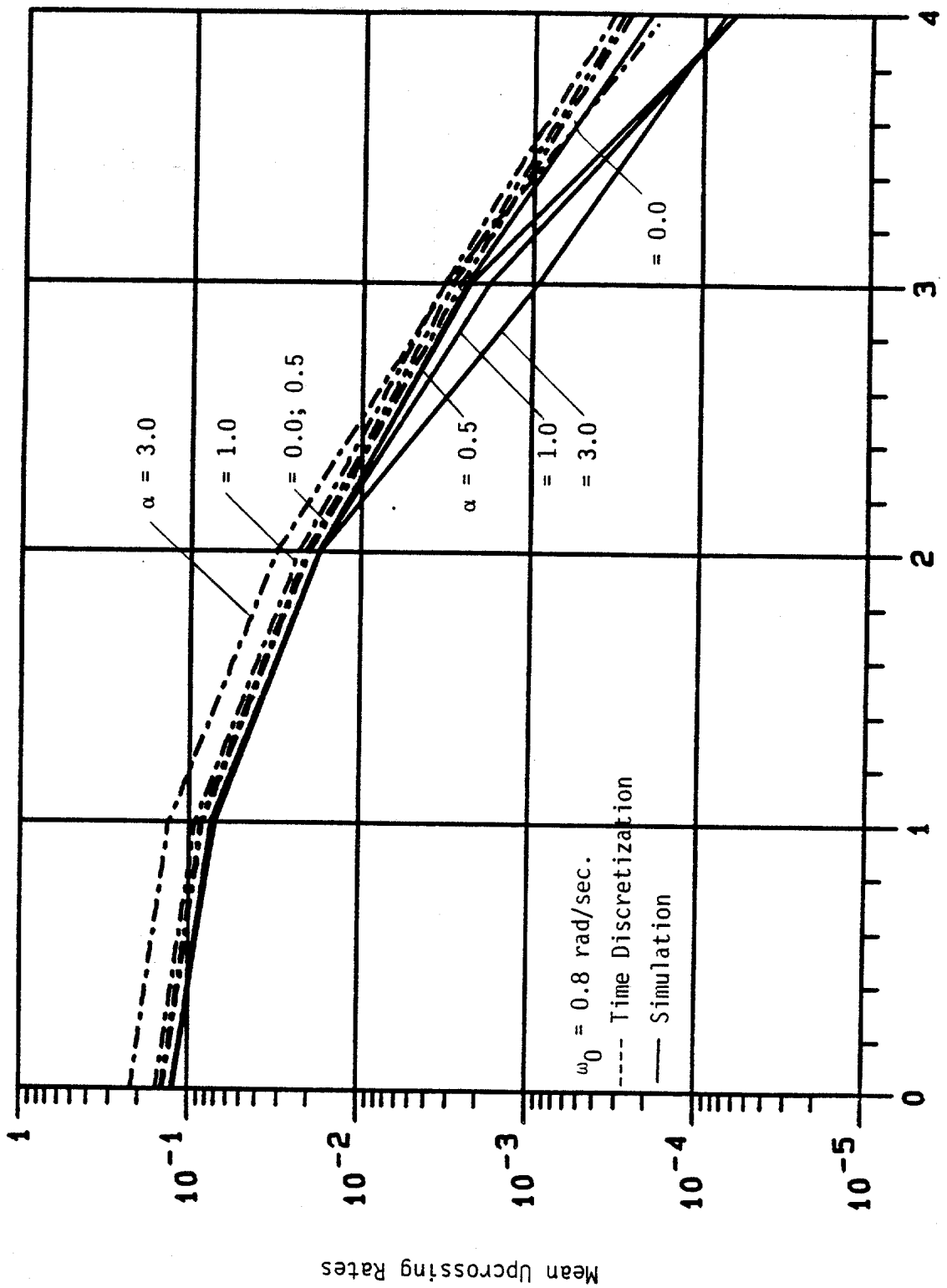

Figure 6(b). Exact and Approximate (Time-Discretization Method) Upcrossing Rates of Dynamic Response.

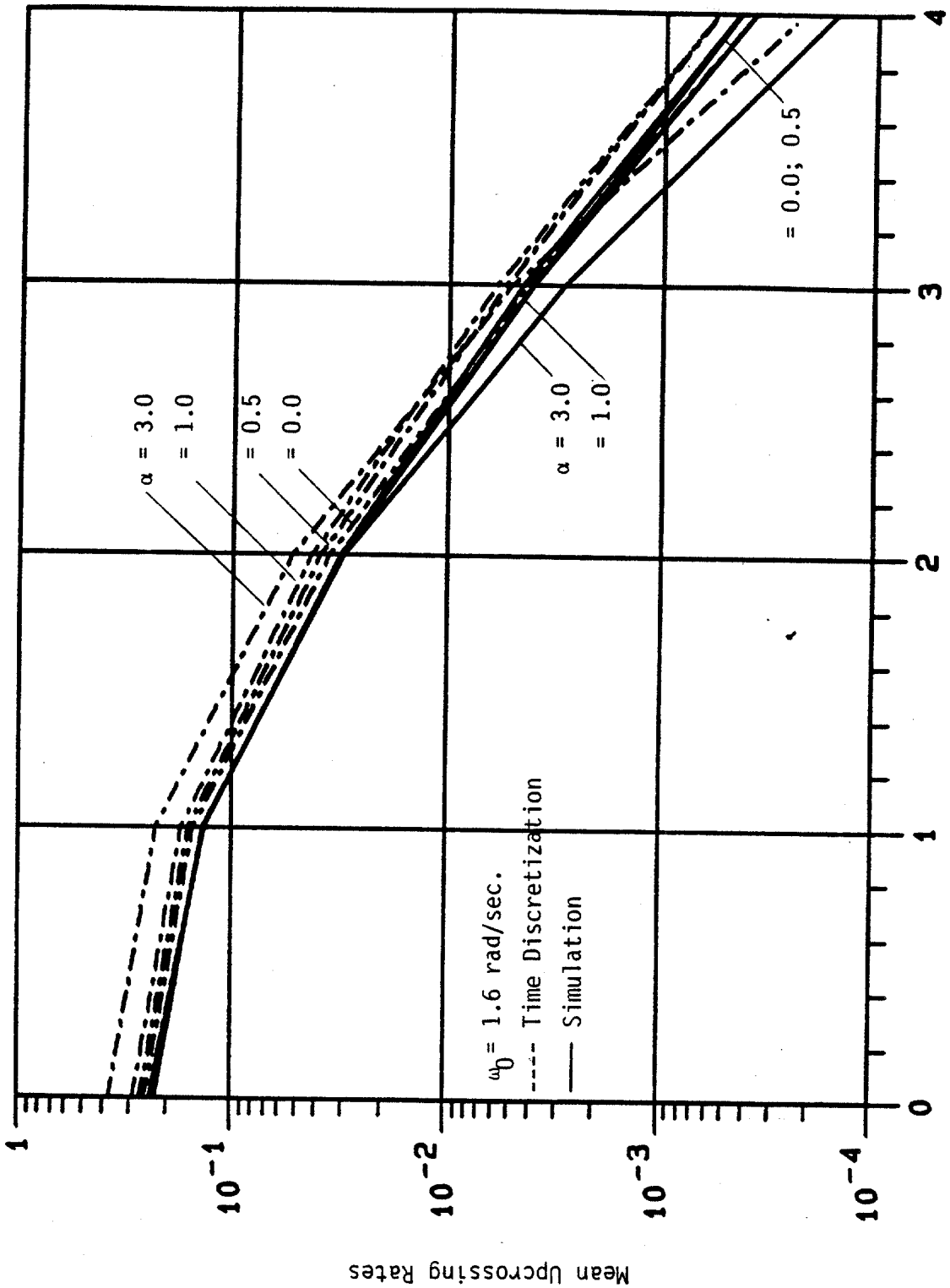

Figure 6(c). Exact and Approximate (Time-Discretization Method) Upcrossing Rates of Dynamic Response.

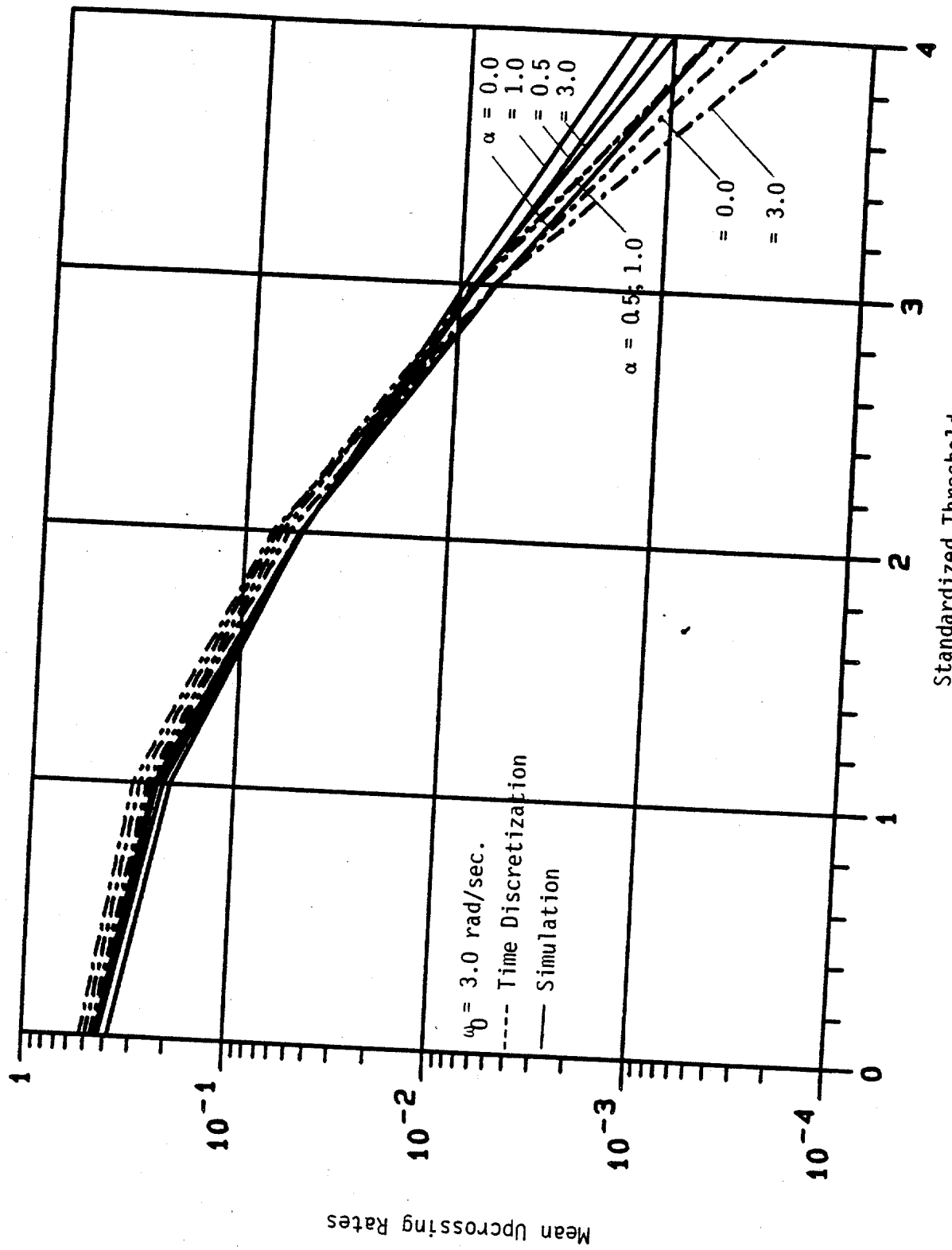

Figure 6(d). Exact and Approximate (Time-Discretization Method) Upcrossing Rates of Dynamic Response.

NBS-114A (REV. 2-8C)

U.S. DEPT. OF COMM. **BIBLIOGRAPHIC DATA SHEET** (See instructions)	1. PUBLICATION OR REPORT NO. NBS/GCR-85/501	2. Performing Organ. Report No.	3. Publication Date SEPTEMBER 1985

4. TITLE AND SUBTITLE

Response of Compliant Offshore Platforms to Waves

5. AUTHOR(S)

Mircea Grigoriu and Bunu Alibe

6. PERFORMING ORGANIZATION (If joint or other than NBS, see instructions)

NATIONAL BUREAU OF STANDARDS
DEPARTMENT OF COMMERCE
WASHINGTON, D.C. 20234

7. Contract/Grant No.

8. Type of Report & Period Covered

9. SPONSORING ORGANIZATION NAME AND COMPLETE ADDRESS (Street, City, State, ZIP)

Minerals Management Service
Reston, VA 22091

10. SUPPLEMENTARY NOTES

☐ Document describes a computer program; SF-185, FIPS Software Summary, is attached.

11. ABSTRACT (A 200-word or less factual summary of most significant information. If document includes a significant bibliography or literature survey, mention it here)

Probabilistic descriptors are developed for the response of structures of the Tension Leg Platform type to current and waves. These are obtained by Monte Carlo techniques by assuming the validity of the Morison equation. The results are compared to those obtained by using statistical linearization techniques. Also, for offshore platforms with higher natural periods of vibration, mean upcrossing rates for various levels of the structural response are estimated by simulation, by statistical linearization techniques, and by additional procedures developed in the report. It is concluded that statistical linearization techniques can underestimate significantly the structural response induced by current and waves.

12. KEY WORDS (Six to twelve entries; alphabetical order; capitalize only proper names; and separate key words by semicolons)

Extreme values; ocean engineering; offshore platforms; random processes; tension leg platforms; wave forces.

13. AVAILABILITY

☒ Unlimited

☐ For Official Distribution. Do Not Release to NTIS

☐ Order From Superintendent of Documents, U.S. Government Printing Office, Washington, D.C. 20402.

☒ Order From National Technical Information Service (NTIS), Springfield, VA. 22161

14. NO. OF PRINTED PAGES

59

15. Price